Received: 20 August 2024 | Revised: 13 November 2024 | Accepted: 24 December 2024

DOI: 10.1002/esp.6066

RESEARCH ARTICLE

ESPL WILEY

Tectonic implications of raised Quaternary relative sea-level indicators along the NE border of the Campania Plain (southern Italy)

Ciro Cerrone[1,2] | Marco Meschis[3] | Alessandra Ascione[2] | Michele Soligo[4] | Paola Tuccimei[4] | Jennifer Robertson[5] | Gerald P. Roberts[5]

[1]Department of Environmental Sciences, Informatics and Statistics (DAIS), University of Venice Ca' Foscari, Venice, Italy

[2]Department of Earth, Environmental and Resources Sciences, DiSTAR, University of Naples Federico II, Naples, Italy

[3]National Institute of Geophysics and Volcanology, Palermo Section, Palermo, Italy

[4]Department of Science, Roma Tre University, Rome, Italy

[5]Department of Natural Sciences, Birkbeck College, University of London, London, UK

Correspondence
Ciro Cerrone, Department of Environmental Sciences, Informatics and Statistics (DAIS), University of Venice Ca' Foscari, Via Torino 155, 30172, Venice, Italy.
Email: ciro.cerrone@unive.it

Funding information
This work was supported by the Italian Association for the Study of the Quaternary (AIQUA) and the Italian Alpine Club (CAI), which awarded Ciro Cerrone of a research grant for Quaternary studies in the central-southern Apennines.

Abstract

Tectonically raised paleoshorelines have been recently identified along the southern fault scarps of the Mt. Fellino and Roccarainola horst blocks, which are part of the northeastern border of the Campania Plain coastal basin (southern Apennines, Italy). Such horst blocks are bounded to the south by the Polvica Fault, a roughly E-W trending normal fault. The sequence of uplifted paleoshorelines has been studied in detail by integrating geomorphological, structural and stratigraphical analyses to assess the Quaternary uplift of the Mt. Fellino and Roccarainola horst blocks. Yet, the staircase of paleoshorelines is still not chronologically well constrained.

Aimed at constraining the uplift history of Mt. Fellino and Roccarainola horst blocks and the rate of activity of the Polvica fault, in this study, we integrate former knowledge on paleoshorelines with a geomorphological analysis to map erosional terraces, that we interpret as remnants of shore platforms. We apply the synchronous correlation method, driven by new and a former $^{230}Th/^{234}U$ dating of calcite veins cutting marine sands, to infer the age of the paleoshorelines and terraces. Based on the synchronous correlation, the mapped paleoshorelines and terraces are correlated with sea-level peaks of the late Early to Late Pleistocene. In particular, the paleoshorelines along the Mt. Fellino ridge are correlated with the Marine Isotope Stage (MIS) 7e and 9c or 11, while the oldest terrace is correlated with the sea-level peak of 980 ka. Using inferred paleoshorelines ages, we estimate the uplift rate of the Polvica Fault footwall. The uplift rate varies from c. 0.2 mm/yr close to the western fault tip up to c. 0.5–0.6 mm/yr in the East, in the Roccarainola block. We combine surface evidence with subsurface data from a shallow well to constrain the vertical throw of the Polvica Fault. A mean fault throw rate of c. 0.4 mm/yr in the last c. 1 Ma is estimated for the central part of the PF. Assuming that the Polvica Fault is still active, we estimate the maximum expected earthquake by means of empirical relationship and obtain a Mw ~ 6.2 value and recurrence interval value of c. 1,200 yr. Historical seismicity activity of the PF has not been acknowledged to date. However, our results raise the crucial question of an in-depth assessment of the seismic hazard for the densely populated Campania Plain.

KEYWORDS
Campania Plain (southern Apennines), coastal geomorphology, Quaternary, raised paleoshorelines, tectonics

1 | INTRODUCTION

The complex interaction between relative sea level fluctuations, tectonic uplift and sedimentary inputs controls the elevation and shape of flights of marine terraces and the formation of Quaternary coastal plains, beach ridges and coral reefs (Chauveau et al., 2024; Lajoie, 1986; Rubio-Sandoval et al., 2021). Rates of coastal uplift have been calculated by studying tectonically deformed flights of marine terraces/coral reefs (e.g., Cerrone et al., 2021a; Chauveau et al., 2021; de Gelder et al., 2022; Decker, Falkenroth, & Hoffmann, 2024; Karymbalis et al., 2022; Ott et al., 2019; Perazzotti, Del Valle, & Fornós, 2024a, 2024b; Roberts et al., 2013; Robertson et al., 2019; Rubio-Sandoval et al., 2024; Saillard et al., 2009). Where active faults affect uplift, these investigations may provide along-strike profiles of fault deformations spanning different timescales (Georgiou et al., 2022). Therefore, crucial insights for an improved long-term seismic hazard assessment related to a seismically deforming region may be inferred. Crustal extension occurring in the southern Apennines is seismically accommodated by active normal faults in the chain, with geodetic and Holocene extension rates in reasonable agreement within a range of 1–2 mm/yr (e.g., Devoti et al., 2017; Faure Walker et al., 2012; Ferranti & Oldow, 2005; Palano et al., 2011; Papanikolaou & Roberts, 2007; Serpelloni et al., 2005, 2022; Sgambato, Faure Walker, & Roberts, 2020). The study area is located in the Campania Plain (Figure 1), a Quaternary coastal graben of the southern Apennines. Here, only low to moderate seismicity has been recorded, and no evidence of surface rupture has been reported over historical times. That led the Database of Individual Seismogenic Sources (DISS3.2.1; DISS Working group, 2018) to indicate no potential seismogenic source both inside and at the boundaries of the Campania Plain. On the contrary, active and capable faults bounding the Campania Plain are reported in the ITHACA (ITaly HAzard from CApable faults) catalogue (ITHACA Working Group, 2019). The Polvica Fault is included among these faults and in ITHACA catalogue it is named as the Cancello Fault and the Sabato Valley-Accellica-Polveracchio Fault. Cinque, Ascione, & Caiazzo (2000) consider the Polvica Fault among the faults which may have slipped in the last 40 ka (i.e., after the eruption of Campania Ignimbrite, dated ~39 ka; Giaccio et al., 2017). The Polvica Fault (hereafter labelled as PF, Figure 1), an ~ E-W trending, S-dipping extensional fault zone with a minimum length of about 15 km located at the southern boundary of Mt. Fellino ridge – Roccarainola horst blocks, is one of the main structures that delineate the NE boundary of the Campania Plain (Cerrone et al., 2021b; Figure 1). According to the Italian Catalogue of Earthquakes (Rovida et al., 2020, 2021), earthquakes with low to moderate magnitude have occurred in historical times in the area around the PF, which has been damaged by the 1,499 "Nola" (Mw 5.6), the 1,561 "Sorrento peninsula" (Mw 5.6) and the 1805 "Piana Campana" (Mw 5.1) earthquakes (Figure 1). An assessment of the PF slip was performed by Cinque, Ascione, & Caiazzo (2000) based on correlation of a marine terrace located at 50 m a.s.l. in the western sector of the Mt. Fellino ridge with marine deposits drilled in the Campania Plain and age ~125 ka by U/Th dating of *Cladocora caespitosa* coral (Romano, Santo, & Voltaggio, 1994). Hence, Cinque, Ascione, & Caiazzo (2000) estimated a displacement of c. 100 m since 125 ka and inferred a mean slip rate of ~ 1 mm/yr for the PF. Such a value is much higher than the long-term mean throw rate of 0.4–0.6 mm/yr in the last c. 1.5 Ma inferred from geomorphological-stratigraphical evidence, i.e. the relationship between the depth of the bedrock age and the timing of the early phases of extension in the Campania graben (Cinque, Ascione, & Caiazzo, 2000).

Despite the above information, relatively poor surface information is available and/or useful to the reconstruction of the displacement history of the faults at the boundaries of the Campania Plain. Such a problem is mostly due to the scarcity of dated markers (i.e., marine terraces), which implies difficulty in quantifying the amount and timing of the vertical motions of the *horst* blocks.

A recent study based on morpho-stratigraphical analysis of raised paleoshorelines and characterisation of the Quaternary fault system has been carried out on the southern slope of Mt. Fellino ridge and Roccarainola hills (Cerrone et al., 2021b). Such new data appears incongruent with former estimates of the PF slip history. Yet, data available to date on the throw and timing of faulting of the PF do not allow a reliable assessment of the PF slip history, an issue that appears of fundamental importance to the assessment of seismic hazards possibly associated with PF.

A classical morphotectonic study (e.g., Parrino et al., 2023; Sorrentino, Valente, & Mondillo, 2023) of the Mt. Fellino ridge, Roccarainola hills area and the adjacent alluvial plain, focused on the study of the mapped paleoshorelines integrated with a detail-scale geomorphological analysis to map erosional terraces was carried out. In this study, we apply a synchronous correlation approach driven by new age controls for a comprehensive analysis of the flight of terraces that are preserved along the Mt. Fellino southern slope, which continues eastwards to the Roccarainola hills (Figure 1). In particular, we refined vertical deformation rates over the late Quaternary for the S-dipping PF, aimed at a better understanding of the relationship between crustal extension and surface uplift in the investigated area. For the investigated region, we attempt to (i) estimate along-strike fault uplift rates, (ii) investigate any spatial variations of fault-related uplift rates, which would confirm the Late Quaternary faulting activity of the PF, (iii) explore along-strike fault rates of tilting through time for marine terraces to estimate gradients of fault displacement and (iv) assess fault throw rates from displaced marine terraces. We discuss our results in terms of tectonic implications and seismic hazard.

2 | GEOLOGICAL AND GEOMORPHOLOGICAL SETTING

The formation of the Campania Plain coastal basin is related to the tectonic evolution of the southern Apennines, a late Tertiary to early Quaternary NE-verging orogenic belt. The Campania Plain, one of the largest coastal basins along the Tyrrhenian side of the southern Apennines, was formed during the early Pleistocene as a result of extensional processes related to the formation of the Tyrrhenian back-arc basin (e.g., Sartori, 1990). It is a NW-SE elongated, rectangular-shaped structural depression of ~2000 km^2 (Figure 1a) with a relatively flat topography interrupted by the Somma-Vesuvius and Campi Flegrei volcanic centres, which experienced significant eruptions in historical times (Barra et al., 1996; Brancaccio et al., 1995; Romano, Santo, & Voltaggio, 1994; Santangelo et al., 2010; Scarpati et al., 2025a; Scarpati et al., 2025b). The geological evolution of the Campania Plain

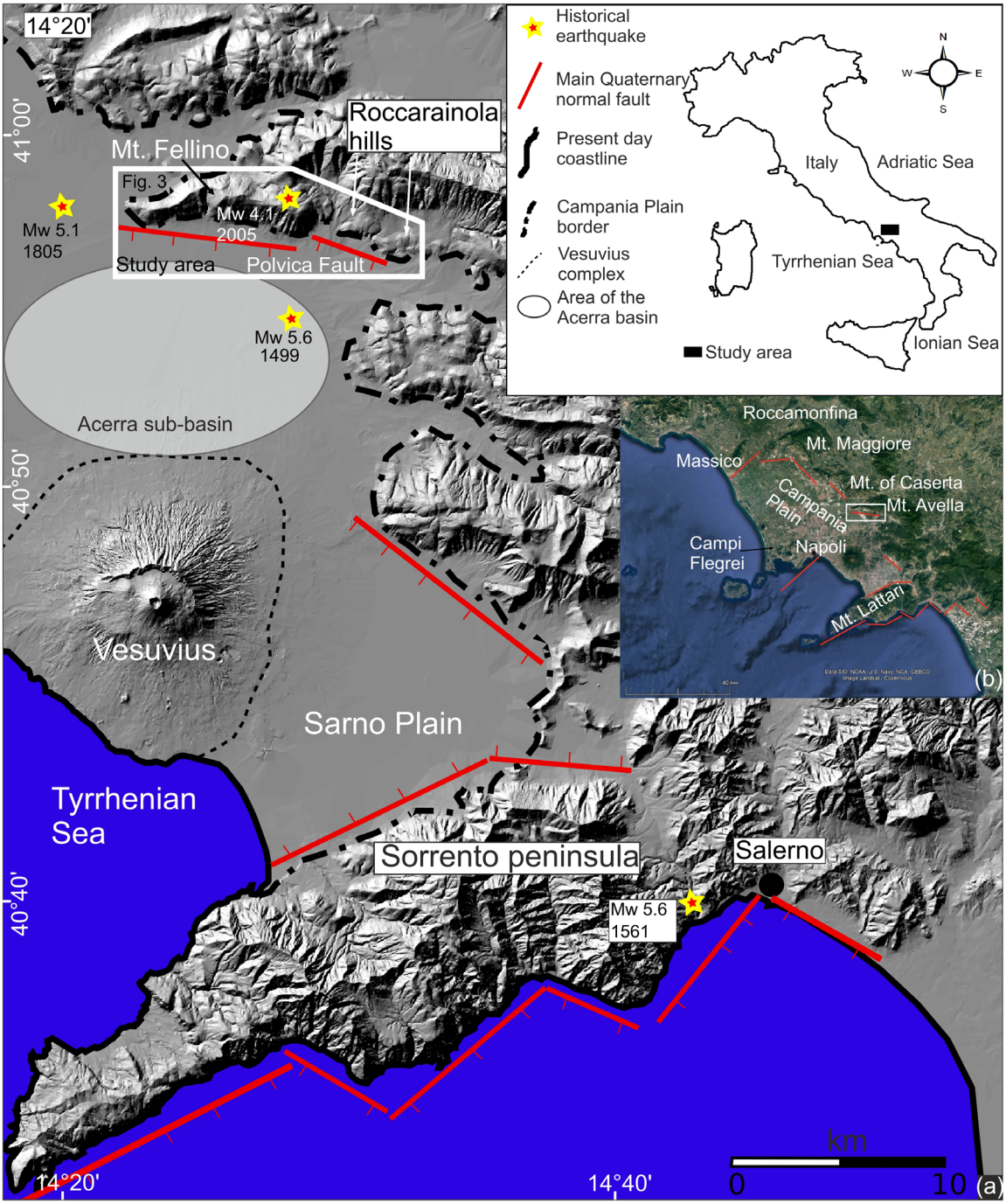

FIGURE 1 (a) Shaded relief of the southern sector of the Campania Plain and surrounding mountains extracted from a 10 m resolution DEM (Tarquini et al., 2007, 2012). In the map, the study area (white polygon) and the location of historical earthquakes from the *Catalogo parametrico dei terremoti italiani 2015 (CPTI15)* (Rovida et al., 2020, 2021) are indicated. A detail of the study area is shown in Figure 3; (b) Google Earth image modified with the main Quaternary faults along the Campania Plain.

has been inferred mostly from subsurface data, e.g., geophysical and deep and shallow well data (Aiello et al., 2021; Amorosi et al., 2012; Barra et al., 1991; Barra et al., 1996; Brancaccio et al., 1991, 1995; Bruno, Cippitelli, & Rapolla, 1998; Cerrone et al., 2021c; Cinque, 1991; Corrado et al., 2024; Florio et al., 1999; Ippolito, Ortolani, & Russo, 1973; Romano, Santo, & Voltaggio, 1994; Santangelo et al., 2010, 2017; Totaro et al., 2024). These investigations show that the carbonate successions that form the backbone of the basin's horst blocks are downthrown in the subsurface of the Campania Plain down to 3,000–4,000 m below the sea level by E-W, NE–SW, NW-SE and N-S oriented high-angle extensional faults, which have produced northward thickening of the basin fill, mainly due to the roughly NE–SW trending master faults (Ippolito, Ortolani, & Russo, 1973; Mariani and Prato, 1988; Florio et al., 1999; Milia & Torrente, 1999, 2015; Caiazzo, Ascione, & Cinque, 2006; Cella et al., 2007; Milia et al., 2013).

The deposits filling the Campania Plain basin consist of Pleistocene to Holocene shallow marine, transitional and alluvial sediments, which are interlayered with volcanic (lava and pyroclastic) deposits supplied by several buried and outcropping eruptive centres (Santangelo et al., 2017 and references therein; Figure 1). Since the Middle-Late Pleistocene, volcanic activity of the Somma-Vesuvius and

Campi Flegrei volcanic complexes provided prominent volcanic inputs into the Campania Plain.

The eastern boundary of the Campania Plain is defined by a series of carbonate ridges striking NW-SE (e.g., Mt. Maggiore and Caserta Mts.) and roughly E-W, such as Mt. Fellino ridge (Figure 1). The PF defines the northern boundary of the so-called Acerra sub-basin (Cella et al., 2007; Florio et al., 1999) of the major Campania Plain (Figure 1). In the Acerra sub-basin several E-W trending extensional faults are identified to the south of PF (Aprile, Sbrana, & Toccaceli, 2004; Bellucci, Santangelo, & Santo, 2003; Scandone et al., 1991).

Holocene tectonic activity has affected the sub-plains of Sarno and Volturno. In the inner sector of the Sarno Plain, geomorphological and stratigraphic evidence of Holocene fault activity has been recognised (Santo et al., 2019; Valente et al., 2019, 2021) and post Campania Ignimbrite motions in the northern Volturno Plain are described by Corrado et al. (2020).

2.1 | Paleoshorelines along Mt. Fellino ridge and Roccarainola hills

Along Mt. Fellino ridge and Roccarainola hills (Figure 1), Cerrone et al. (2021b) identified three distinct paleoshorelines labelled T1, T2 and TRR, characterised by shore platforms covered by transgressive-regressive sedimentary wedges (Figure 2). These include shallow marine deposits, e.g., conglomerates and sands/arenites bearing fossiliferous contents (bivalves and microfossils). The highest paleoshoreline (TRR, Figure 2e) has been identified just in the eastern part of the study area, in the Roccarainola hills (Figure 1).

Such paleoshoreline, labelled TRR in Cerrone et al. (2021b), consists of a wave-cut platform located ~ 200 m a.s.l. and covered by a matrix-supported conglomerate composed of well-rounded pebbles, which passes upwards to a few decimetres thick sandy deposits containing benthic foraminifera (Cerrone et al., 2021b; Figure 2). The marine deposits of the TRR are generally covered by a few metre-thick colluvium.

The T1 and T2 paleoshorelines consist of terrace remnants that crop out rather continuously along Mt. Fellino southern slope. However, both the elevations of the T1 and T2 wave-cut platforms and their vertical separation vary spatially along Mt. Fellino ridge, decreasing from the centre of the PF towards its western tip (Cerrone et al., 2021b). Mutual correlation between remnants of the T1 and T2 is based on the stratigraphic and geomorphological features (e.g., sizes of the abrasion platforms, sedimentary facies and thicknesses of the deposits overlying the abrasion platforms; Cerrone et al., 2021b).

The elevation of the T1 platform inner margin ranges from 80 m, in the centre of the Mt. Fellino ridge, to 50 m a.s.l. in the western part of the ridge. The T1 abrasion platform is covered by a few metre-thick shallow marine deposit composed, from the bottom, of conglomerates passing upward to calcarenites bearing bivalve shells and shell casts (Figure 2). The marine deposits are overlain by either alluvial fan or colluvial deposits containing abundant reworked volcanic material (Figure 2).

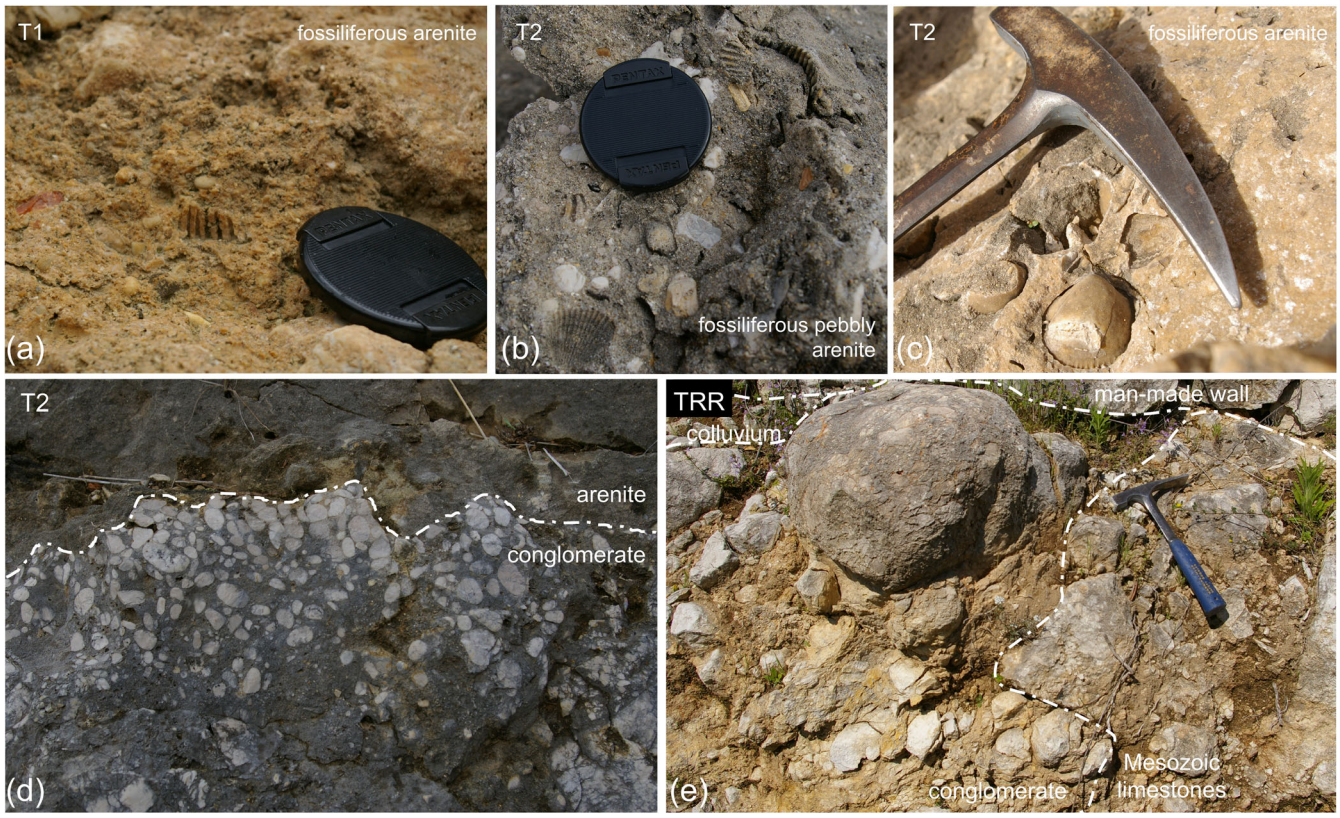

FIGURE 2 Images of the deposits associated with paleoshorelines T1, T2 and TRR. (a) Arenite with pebbles and bivalve remnants of paleoshoreline T1. (b,c) Arenites and pebbly arenites with bivalve fragments and casts of paleoshoreline T2. (d) Conglomerate passing upwards to arenite of paleoshoreline T2. (e) Coarse conglomerate with a sandy matrix of paleoshoreline TRR.

The elevation of paleoshoreline T2 ranges from 70 to 115 m a.s.l. The deposits associated with the T2 are composed of a basal conglomerate which grades upwards into shoreface deposits with bivalves and benthic fauna (Cerrone et al., 2021b; Figure 2). At some outcrops, large rock-fall deposits resting onto the shore platform testify to sea-cliff retreat during the platform formation (Cerrone et al., 2021). The marine deposits are covered by coarse-grained continental deposits several metres thick. The T2 is displaced by S-dipping normal faults and N to NNW striking, oblique-slip transfer faults. Tension fractures affect the T2 deposits and extension veins are distributed subparallel to the main normal faults and transfer faults. The veins contain calcite, typically present in the form of blocky crystals. Calcite veins related to fault-fluid interactions (e.g., Li et al., 2020), are frequently found dispersed throughout carbonate rocks within fault zones.

Based on the dating of a calcite vein (sample C.PI2) dissecting the shoreface deposits of T2, Cerrone et al. (2021b) assigned to paleoshoreline T2 an age > MIS 7 and hypothesized a correlation with MIS 9. Based on sequential correlation criteria, the Authors hypothesised a correlation of T1 and TRR with MIS 7 and MIS 11, respectively.

3 | MATERIALS AND METHODS

The geomorphological setting of Mt. Fellino and Roccarainola hills was reconstructed by analyses of topographic data using 1:5000 scale maps, a 5 m resolution-Digital Elevation Model (DEM) released by the Regione Campania (Figure 3) and a 1 m resolution (LiDAR) DEM released by the Italian Ministry of Environment (MITE). The marine terrace data have been modelled by the synchronous correlation method driven by new and already published age controls to reconstruct the Quaternary uplift rate of the area (e.g., Houghton et al., 2003; Roberts et al., 2009, 2013; more details in Section 3.1).

The reconstructed long-term uplift of the PF footwall block was used in combination with subsurface data to estimate the PF throw.

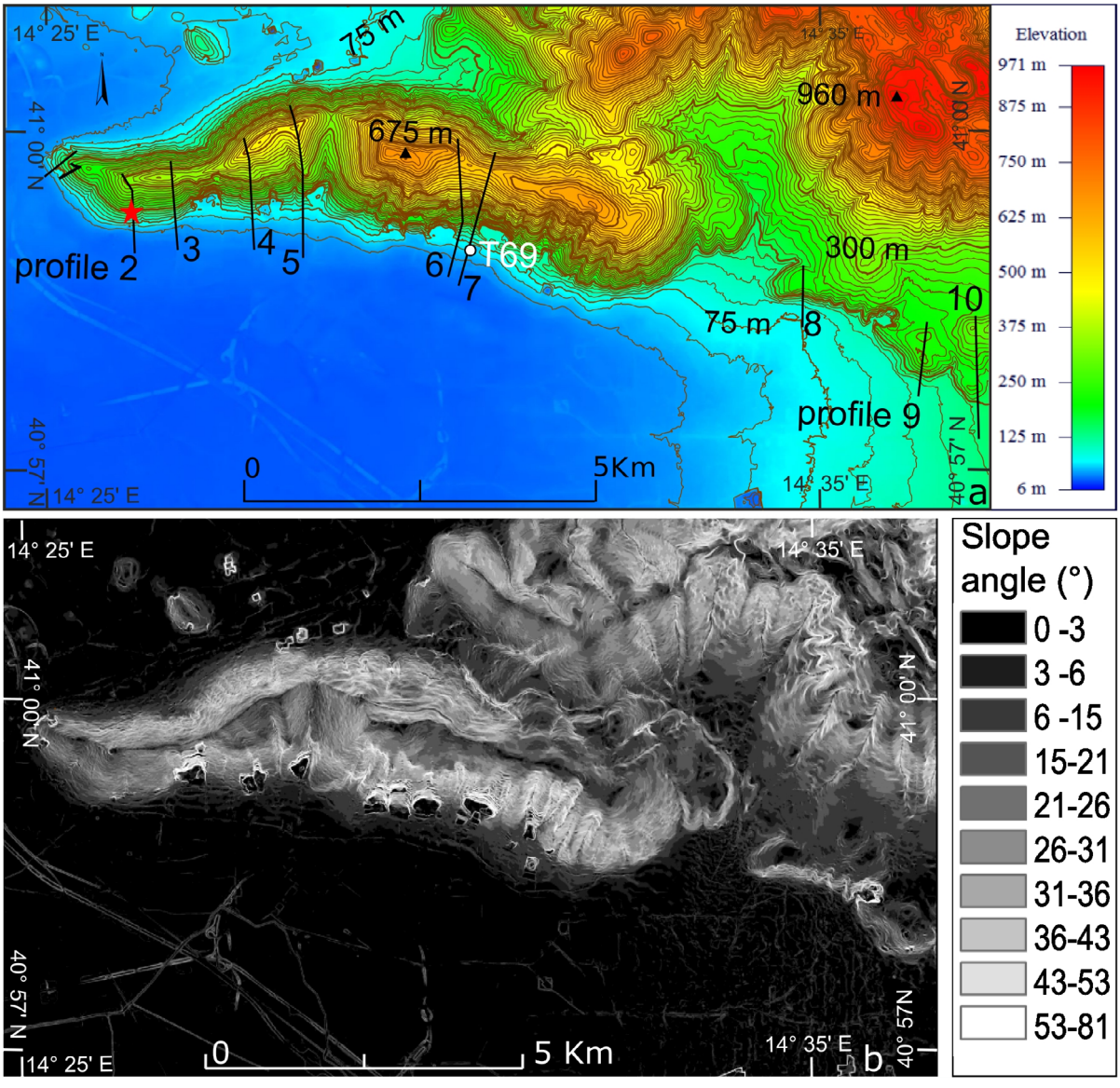

FIGURE 3 The 5 m resolution DEMs of the Mt. Fellino ridge and Roccarainola hills. (a) Elevation map with 15 m contour lines. In the map, the traces of the 10 topographic profiles are reported. The red star indicates the location of the sampled calcite vein; (b) slope angle map of Mt. Fellino ridge and Roccarainola hills in degrees.

To constrain the throw, we used the stratigraphic log of a shallow borehole (T69 borehole; location in Figure 3; Figure S1) located in the hanging wall block of the PF (location in Figure 3). As a final step, we used information on the PF geometry inferred from our study to estimate the possible maximum expected earthquake magnitude of the PF by means of the empirical relationship between the fault length and magnitude first proposed by Wells & Coppersmith (1994). To evaluate the magnitude, we applied the formula ($Mw = 4.7248\ L\ [km]^{0.1046}$) by Galli, Galadini, & Pantosti (2008).

3.1 | The synchronous correlation method

The synchronous correlation method developed by Houghton et al. (Roberts et al., 2009, 20,132,003) and Roberts et al. (2009) has been applied in several studies over the last decade (e.g., De Santis et al., 2023; Meschis et al., 2018, 2020, 2022; Pedoja et al., 2018; Robertson et al., 2019, 2023). This method is based on the concept that, for a given constant uplift rate, Quaternary sea-level highstands producing raised sea-level indicators are unevenly spaced in time, implying that preserved paleoshorelines are unevenly spaced in elevation. The adaptability of this approach is shown when it is applied to scenarios with either constant or fluctuating uplift rates as demonstrated by previous investigations (e.g., Meschis et al., 2018, 2022; Roberts et al., 2009; Varzi et al., 2024). This method overcomes the "re-occupation" problem of younger sea-level indicators over older ones, avoiding assigning erroneous relative ages to undated marine terraces when regions with relatively low uplift rates are investigated (e.g. De Santis et al., 2023; Robertson et al., 2019). For this approach, given that at least one age control is obtained for a paleoshoreline, the simplest hypothesis of having a constant uplift rate through time is tested, iterating values of uplift rates driven by available age controls (e.g., Meschis et al., 2018, 2022; Roberts et al., 2013 and references therein). Such a process enables the user to iteratively calculate sea level highstand elevations driven by age controls which may be either newly obtained absolute dating or well-known literature. This allows the assessment of whether the predicted/modelled elevations of marine terraces of different ages match the elevations of mapped paleoshorelines (e.g., Meschis et al., 2018). If there is not a robust match between mapped and predicted elevations, then scenarios with uplift rates varying through time are tested, as shown by previous investigations (e.g., Meschis et al., 2022; Roberts et al., 2009).

In our case study, the dataset used for the modelling includes (i) paleo sea-level indicators, i.e., shoreline angles of well-developed marine-built terraces, hereinafter labelled paleoshorelines, namely T1, T2 and TRR (Section 2) (Figure 4), and (ii) marine-cut/erosional terraces, hereinafter labelled terraces, cutting the carbonates of the southern slope of Mt. Fellino ridge and Roccarainola hills. The erosional terraces were identified through the geomorphological analysis

FIGURE 4 Images of paleoshorelines T1 (a) and T2 (b), with the indication of the platform shoreline angles. The outcrop in image (a) is located in the western part of Mt. Fellino ridge (profile 2, location in Figure 3); image in (b) is located in the central part of Mt. Fellino ridge (profile 6, location in Figure 3).

TABLE 1 Elevation (m a.s.l.) of T1, T2 and TRR shoreline angles along profiles 1 to 10. The location of the profiles is reported in Figure 3.

	Paleoshoreline elevations (m)		
Profile numbers	T1	T2	TRR
1		70	
2	50	75	
3		105	
4		115	
5		115	
6		110	
7		110	
8			200
9			200
10			200

of the topographic data. In the modelling, the terraces were interpreted as eroded remnants of shore platforms. Such an assumption was based on the terraces' shapes, which are flat to slightly south-dipping (i.e., dipping towards the sea) and, therefore, suggestive of a marine origin for the terraces.

For paleoshorelines T1, T2 and TRR, the elevations of the platform's shoreline angles, which were used in the modelling, were both measured by a handheld GPS receiver and inferred from topographic (DEM) data. The double estimations of the paleoshoreline elevations served us to test by means of regression analysis the reliability of the DEM-based topographic analysis.

DEM-based values of the terraces' elevations were used as input data for the modelling. The elevation error range of the DEM-based values is in metric order, which is in line with the decametric uncertainties within the sea-level curves used in this work. Using ArcMap 10.4 software, 10 topographic profiles (labelled 1 to 10 from the west to the east; Figure 3a) were constructed across the southern escarpments of Mt. Fellino and Roccarainola hills, intercepting paleoshorelines T1, T2 and TRR and the DEM-mapped terraces. The 10 profiles were used for the synchronous correlation analysis. The elevations of the shoreline angles of paleoshorelines T1, T2 and TRR along the 10 profiles are reported in Table 1.

Global sea-level curves used for the modelling are curves by Siddall et al. (2003) for the < 410 ka time range, and by Rohling et al. (2014) for > 411 ka times (Table S1).

It is important to note that data from different sea-level curves may imply variations in modelled paleoshoreline elevations. However, Robertson et al. (2019) showed that the overall spatial uplift pattern and uplift rates did not vary too greatly when data from different sea-level curves were used in the modelling.

To support the synchronous correlation modelling we used independent age constraints (Section 3.2). To assess the correlation between elevations of measured and predicted paleoshorelines, linear regression analysis was carried out, aiming at maximizing the coefficient of determination (R^2), similar to previous investigations (e.g., Roberts et al., 2013; Varzi et al., 2024). For clarity, in the following Sections we will use the terms: (i) paleoshoreline, to indicate the marine-built terraces T1, T2 and TRR (Section 2); (ii) terrace, to indicate erosional terraces mapped by DEM analysis; (iii) predicted sea-level position when referring to the present elevation of an uplifted sea-level indicator of a certain age inferred from the synchronous correlation modelling.

3.2 | Age constraints

Our synchronous correlation modelling is driven by independent age constraints from an existing (Cerrone et al., 2021b) and a new U-series dating (Table 2; samples location in Figure 3a). The dated samples are from two calcite veins dissecting the shoreface deposits associated with the paleoshorelines T2. Continental carbonate deposits, such as calcite veins, are considered suitable for U-Th dating if (i) the initial content of uranium is sufficient for measurements and (ii) none, or very limited, detrital thorium component is present in the analysed sample. U-series method is based on the fractionation of ^{238}U and ^{234}U to the daughter nuclide ^{230}Th. Samples (around 30 g) were powdered and dissolved in nitric acid at the University Roma Tre facilities, with the addition of a spike solution containing ^{228}Th and ^{232}U in secular equilibrium. After oxidation of the organic matter with hydrogen peroxide at 100°C, the isotope complexes of uranium and thorium were separated and purified by ion-exchange resin and liquid–liquid extraction techniques (Edwards et al., 1987). Activity ratios were then alpha-counted in a high silicon surface barrier and the age was calculated using Isoplot/Ex (version 3.0), a plotting and regression program for radiogenic-isotope data (Ludwing, 2003).

4 | RESULTS

4.1 | Geomorphological analysis and age constraints

The Polvica fault zone marks the boundary between the elevations of Mt. Fellino ridge – Roccarainola hills and the inner part of the Campania Plain, where the Polvica village is settled (Figure 5). At the junction between the Holocene alluvial plain and the Mt. Fellino ridges in the N, Late Pleistocene–Holocene alluvial fan deposits form a rather continuous surface gently sloping down to the alluvial plain surface (Figure 5). To the S of Mt. Fellino, the plain surface is quasi-flat, ranging from c. 30 m of elevation in the west to 40 m in the east. More to the east, the plain surface, which here is underlain by alluvial deposits delivered by west-flowing rivers that dissect the mountain belt in the E, rises gently to reach c. 100–130 m a.s.l. to the S of the Roccarainola hills (Figure 3).

Information on the stratigraphy of the Polvica plain is inferred from the log of a 200 m deep borehole (T69 borehole, location in Figures 3 and 5; Figure S1) drilled at 34 m a.s.l. in front of the central sector of Mt. Fellino escarpment. The T69 borehole reaches the top of the carbonate bedrock at 116 m below the sea level. The carbonate bedrock is overlain by a c. 70-m thick sandy and gravelly marine deposit (unit b; Figure S1), which is covered by alluvial deposits alternated with pyroclastic/volcanoclastic deposits, which have a cumulative thickness of 49 m. Published borehole data around the study area indicate that the depth of the carbonate bedrock increases towards the S, in the central part of the Polvica plain (Bellucci, Santangelo, & Santo, 2003).

TABLE 2 Uranium contents (mg/g), activity ratios and $^{230}Th/^{234}U$ ages of the analysed calcite veins dissecting the T2 paleoshoreline (1σ).

Sample ID	Locality	Sample type	^{238}U [mg/g]	1σ	$^{234}U/^{238}U$	1σ	$^{230}Th/^{234}U$ meas	1σ	$^{230}Th/^{232}Th$	1σ	Age (ka)	1σ	$^{234}U/^{238}U$init	1σ	Long.	Lat.	References
C.Pl2	Polvica	calcite vein (T2)	0.159	± 0.003	0.995	± 0.016	0.943	± 0.020	158.124	± 8.957	316.0	87/ - 53	0.998	± 0.039	14°26′24.44″E	40°59′12.91″N	Cerrone et al., 2021b
C.Pl3	Polvica	calcite vein (T2)	0.173	± 0.007	0.999	± 0.003	0.725	± 0.041	147.589	± 21.293	141	± 16	0.998	± 0.051	14°26′25.86″E	40°59′12.99″N	unedited data

In front of the central part of Mt. Fellino ridge, the toe of the piedmont is characterised by an elongated, depressed area, lying a couple of metres below the surface of the adjacent part of the Polvica plain and where, according to local people, a marshy environment establishes during the wet season (marsh area in Figure 5). Accordingly, data from unpublished shallow boreholes (around 20 m in depth) point to the occurrence, in the shallow subsurface, of some metres of fine-grained deposits rich in organic matter, consistent with the persistence of a marshy environment in that area. The presence of such a localized marshy area may suggest recent subsidence of the Polvica plain and, therefore, motions along the PF continuing during the Holocene.

Topographic analysis indicates that the steep profiles of the southern escarpments of Mt Fellino ridge and Roccarainola hills are also characterised by the presence of several terraced surfaces, which span in elevation from c. 50 m to > 300 m. These consist of erosional terraces cutting the Mesozoic limestones and might represent remnants of eroded shore terraces. In the text, we use the term terrace to refer to these erosional surfaces without sedimentary cover (Section 3.1).

Age constraints to the undated paleoshotelines/terrace sequence of the Mt. Fellino ridge may be inferred from $^{230}Th/^{234}U$ dating of two calcite veins, which dissect the arenites of paleoshotelines T2 in the western part of Mt. Fellino ridge. In this sector of the ridge, the T2 has an elevation of 75 m a.s.l. (profile 2 in Figure 3; Table 1). The U-series ages of the two calcite vein samples are (i) 316 + 87/− 53 ka for sample C.Pl2 (Cerrone et al., 2021b), and (ii) 141 ± 16 ka for sample C.Pl3 (Table 2).

The age of the oldest calcite vein (sample C.Pl2, Figure 6 and Table 2) spans between 403 and 263 ka, exhibiting a large and asymmetric range of uncertainty primarily attributed to its proximity to the upper limit of the method. Age of sample C.Pl3 (Figure 6 and Table 2) has a relatively small uncertainty range spanning between 125 ka and 157 ka. The age of sample C.Pl3 and the maximum age of C.Pl2 indicate that deformation along Mt. Fellino mountain front occurred at several stages and lasted (considering the uncertainty range) at least from 403 ka to 125 ka. In particular, this time range indicates the time during which there was interaction between the fault-fluid and fractures of the PF fault zone. Since the calcite veins postdate the T2 arenite, it results that the T2 paleoshoreline, considering the minimum age of the oldest calcite vein, was formed at least before 263 ka. Furthermore, such minimum age allowed a constraining T1 < 263 ka.

4.2 | Synchronous correlation approach applied to the marine terrace sequence along Mt. Fellino ridge and Roccarainola hills

To correlate undated paleoshorelines and terraces detected along the southern slope of Mt. Fellino with Quaternary sea-level highstands, we applied the synchronous correlation approach between multiple marine terraces and multiple predicted sea level highstands elevations by iterating uplift rate (Section 3 and Figure 7). Uplift rate values have been iterated in order to find the best match between the elevation of predicted indicators and mapped paleoshorelines/terraces. The synchronous correlation approach, constrained by the U-series dating, allows us to refine ages for all mapped yet undated paleoshorelines

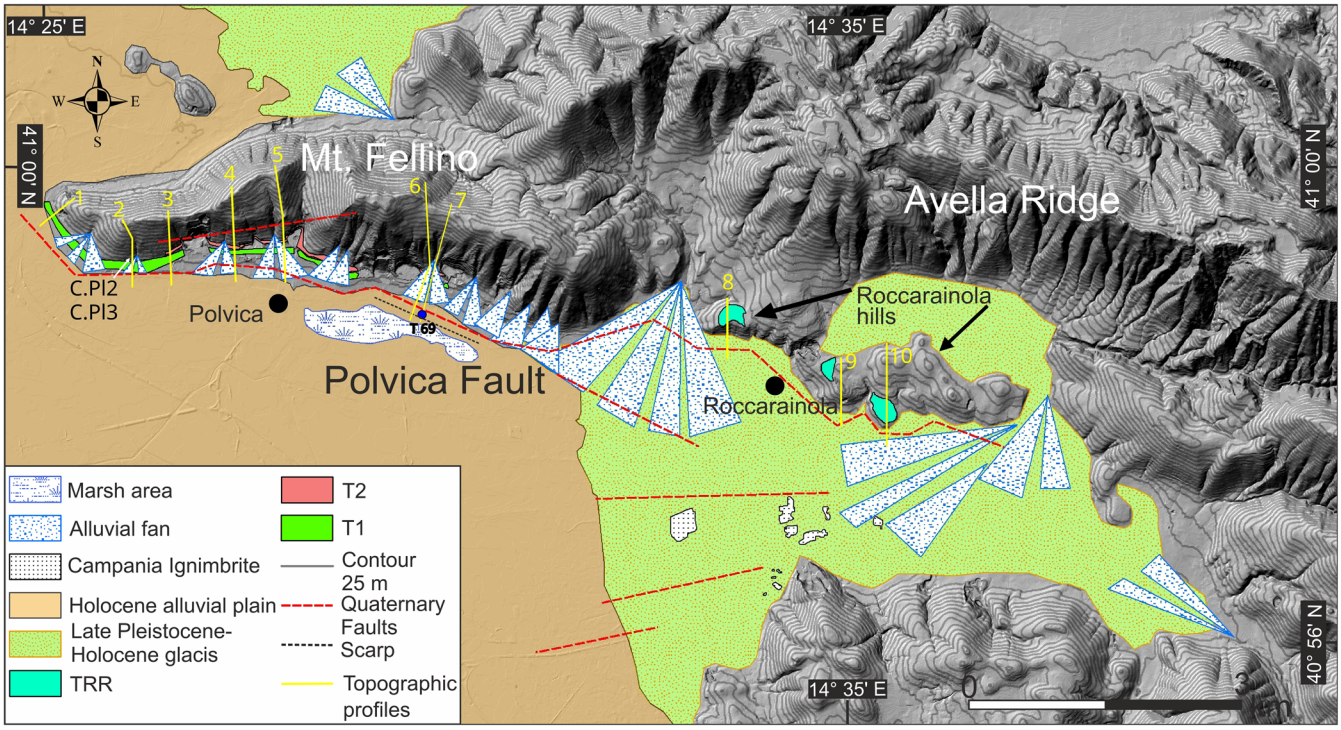

FIGURE 5 Geomorphological sketch of the Mt. Fellino ridge and the Polvica plain, with the indication of paleoshorelines T1 and T2 (along the Mt. Fellino ridge) and TRR, located at c. 200 m in the Roccarainola hills (modified after Cerrone et al., 2021b). In the map are indicated the locations of the topographic profiles 1 to 10, the T69 borehole and the sampling site of the calcite veins (samples C.PI2 and C.PI3).

FIGURE 6 T2 paleoshoreline and close-up view of the marine deposits associated with T2 along profile 2 (Figure 3a). The arenite deposit of T2 is dislocated by E-W and NNW striking normal and transfer faults respectively. The faults are filled by calcite veins which postdated the formation of the marine deposits. (a) Detail of the marine arenite faulted by conjugate high angle normal faults filled by calcite veins; (b) close-up view on the calcite sample label C.PI2 used previously for U-series dating (Table 2); (c) the shore platform T2 at 75 m a.s.l. on profile 2 (Figure 3a) is dissected by NNW striking transfer faults; (d) T2 wave-cut platform cutting the bedrock constituted by Mesozoic limestones and associated marine deposits. The succession is closed by alluvial fan deposits and finally Holocene colluvium (e); (f) close-up view on the calcite sample label C.PI3 (new U-series data, Table 2).

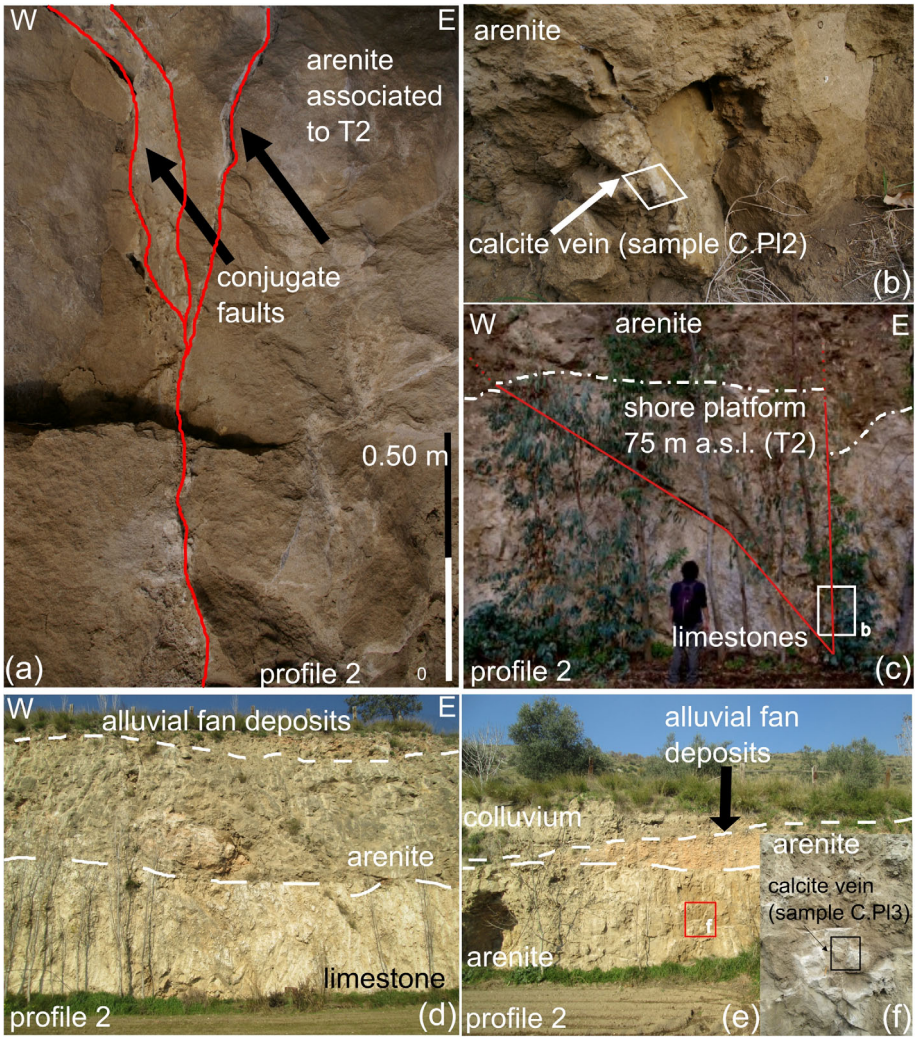

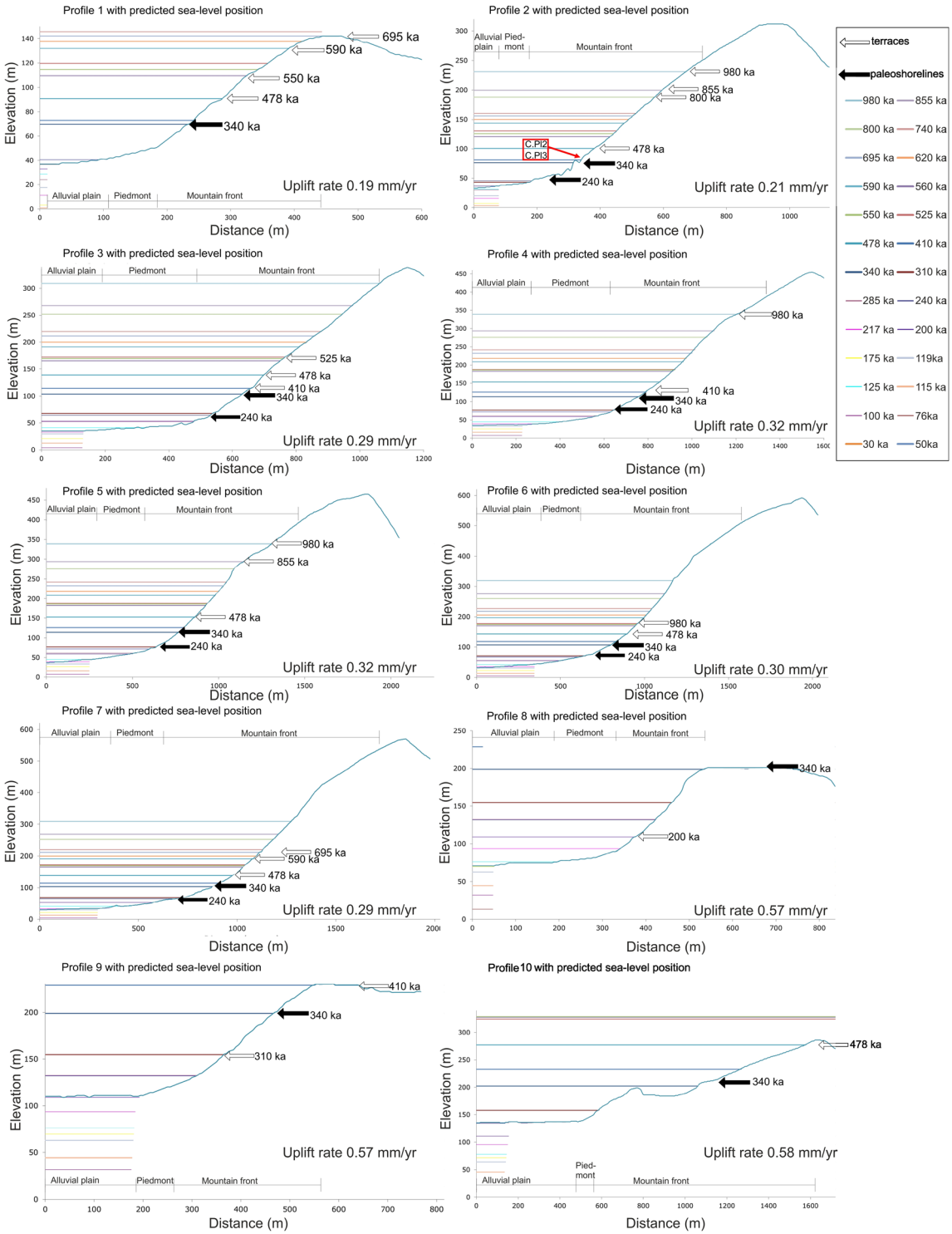

FIGURE 7 Topographic profiles were constructed across Mt. Fellino ridge (1 to 7) and Roccarainola hills (8 to 10; locations are in Figure 3a). The figure shows the case in which TRR is coeval with T2. In the profiles, coloured lines (see the legend for keys to the colours) indicate the sea-level elevations predicted by the modelling; the age of the sea-level peaks are from Siddall et al. (2003) and Rholing et al. (2014) (section 3). The black arrows indicate the positions of the paleoshorelines T1, T2 and TRR; the white arrows indicate elevations of the DEM-mapped terraces. The location of the samples C.Pl2 and C.Pl3 is reported along with profile 2 on the T2 paleoshoreline. Note that (i) there are predicted terraces located below the mountain front-piedmont/alluvial fan junction; (ii) in this figure for the Roccarainola hills is reported the output of the case, where the paleoshoreline labelled TRR, outcropping in Roccarainola area, coincides with T2 paleoshorelines outcropping along the southern side of Mt. Fellino. The arrows indicate the positions of the mapped terraces with predicted ages.

and terraces (Figure 7; Table 3). Assigning (i) an age > 263 ka to the T2 paleoshoreline at 75 m a.s.l. in profile 2, (ii) an age < 263 ka to the T1 at 50 m a.s.l. in profile 2 (Section 2.1; Figure 7 and Figure 8) and (iii) by iteration of uplift rate along the PF on all the paleoshorelines and terraces mapped (Figure 8, Table 3), results that the best match between the elevation of predicted vs. mapped

TABLE 3 Input data (elevations of paleoshorelines and terraces) and results of the synchronous correlation approach based on the assumption that TRR is coeval with T2.

Profile number	Paleoshoreline and terrace label	Latitude (decimal degrees)	Longitude (decimal degrees)	DEM-based elevation of terraces (m)	GPS-based paleoshoreline elevation (m)	Predicted Sea level position (m a.s.l.)	Inferred age (ka)
1	4	40.994588°	14.422711°	70	70 (T2)	70	340
1	6	40.994725°	14.424018°	90	-	91	478
1	8	40.994836°	14.424799°	115	-	115	550
1	9	40.994926°	14.425576°	134	-	132	590
1	10	40.995128°	14.426087°	142	-	142	695
2	2	40.985881°	14.438716°	49	50 (T1)	45	240
2	4	40.986846°	14.438104°	66	75 (T2)	76	340
2	5	40.986923°	14.438089°	91	-	81	410
2	6	40.987401°	14.438022°	105	-	100	478
2	11	40.988950°	14.437684°	177	-	188	800
2	12	40.989254°	14.437773°	199	-	200	855
2	13	40.989943°	14.437517°	242	-	231	980
3	2	40.987656°	14.446634°	62	70 (T1)	65	240
3	4	40.988545°	14.446315°	-	105 (T2)	104	340
3	5	40.988731°	14.446244°	116	-	114	410
3	6	40.989075°	14.446145°	140	-	139	478
3	7	40.989656°	14.445933°	174	-	172	525
4	2	40.988070°	14.458063°	78	80 (T1)	72	240
4	4	40.989245°	14.457991°	-	115 (T2)	114	340
4	5	40.989312°	14.457927°	120	-	126	410
4	13	40.993023°	14.457600°	339	-	339	980
5	2	40.988667°	14.465961°	74	75 (T1)	77	240
5	4	40.989886°	14.466097°	-	115 (T2)	114	340
5	6	40.990763°	14.466074°	149	-	153	478
5	12	40.993736°	14.465477°	285	-	294	855
5	13	40.994595°	14.465391°	320	-	339	980
6	2	40.984582°	14.492035°	75	75 (T1)	67	240
6	4	40.985860°	14.492818°	104	110 (T2)	107	340
6	6	40.986572°	14.492730°	142	-	143	478
6	13	40.989041°	14.492181°	330	-	319	980
7	2	40.983981°	14.495553°	64	70 (T1)	65	240
7	4	40.985601°	14.495902°	-	110 (T2)	104	340
7	6	40.986504°	14.495949°	143	-	139	478
7	9	40.987231°	14.495860°	192	-	191	590
7	10	40.987496°	14.495958°	213	-	212	695
8	1	40.976875°	14.550368°	110	-	109	200
8	4	40.978866°	14.550763°	201	200 (TRR)	199	340
9	3	40.967386°	14.571026°	157	-	155	310
9	4	40.968201°	14.571423°	201	200 (TRR)	199	340
9	5	40.968689°	14.571796°	230	-	229	410
10	4	40.965434°	14.579023°	199	200 (TRR)	202	340
10	6	40.973599°	14.579266°	286	-	277	478

palaeoshorelines is obtained by correlating T2 with the highstand of 340 ka (Figure 8; Table 3), which corresponds to the MIS 9c peak (e.g., Siddall et al., 2003).

Based on the modelling output, paleoshoreline T1 (located 50 m a.s.l. in profile 2; Figure 8) is correlated with the 240 ka sea-level peak (MIS7e, Siddall et al., 2003; Figure 7, Table 3).

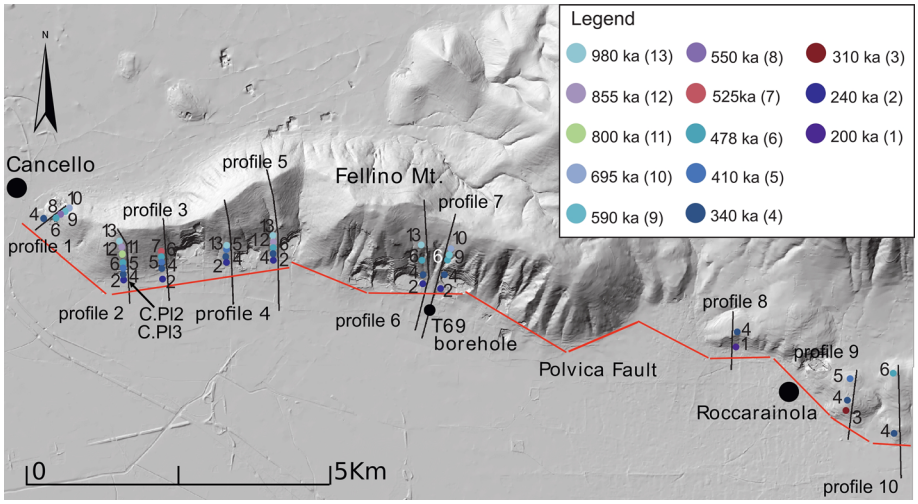

FIGURE 8 Hillshade map with the location of paleoshorelines and terraces along the Mt. Fellino ridge and the Roccarainola hills. The traces of the 10 topographic profiles, used for the synchronous correlation analysis, and the location of the T69 borehole are shown. The paleoshorelines' and terraces' labels, ordered chronologically from the youngest (1) to the oldest (13) as in Table 3, are reported in the map and in the legend (in brackets), along with their modelled ages. Note that the figure shows the output of the case where the age of TRR equals the T2 age.

For Roccarainola hills, where no direct constraint to the age of the paleoshorelines/terraces is available and where the staircase is composed of a few terraces, the correlation with the sea-level peaks is less straightforward than in the Mt. Fellino case. We tested two cases: (i) the hypothesis of having TRR coeval with T2 (Figure 7), which is supported by geomorphological evidence (i.e., sizes of the abrasion platforms) and (ii) the Cerrone et al. (2021b) hypothesis that TRR is correlated with MIS 11 (Section 2.1).

Besides paleoshorelines T1 and T2, the terraces identified by topographic analysis may be associated with positive sea level peaks of the late Early to Middle Pleistocene (Figure 7, Figure 8 and Table 3). Hence, assuming that TRR is coeval with T2, this study has identified marine terraces associated with sea-level highstands 200 ka (1); 240 ka (2); 310 ka (3); 340 ka (4); 410 ka (5); 478 ka (6); 525 ka (7); 550 ka (8); 590 ka (9); 695 ka (10); 800 ka (11); 855 ka (12) and 980 ka (13), not all mapped within a single profile (Figure 8 and Table 3).

To test the reliability of our correlation method, we applied a linear regression analysis to the data sets.

The reliability and robustness of our topographic analysis on 5-m resolution DEM are indicated both by (i) the prominent correlation that exists between the GPS-based and DEM-based paleoshorelines (Figure 9a), and (ii) the correlation between the elevation of the DEM-mapped paleoshorelines/terraces and the predicted sea-level position (Figure 9b). The two correlations are assessed by linear regression with values of R^2 close to 1. It is worth noting that the elevations of both the paleoshorelines and terraces match with the modelling output. Such a match supports our hypothesis of a marine origin for the terraces. Overall, our results indicate that reliable estimates of uplift rates have been gained.

The agreement between predicted and measured paleoshorelines and terraces elevations demonstrated by the linear regression analysis (Figure 9) supports our hypothesis that, along each of the analysed profiles, the uplift rate has been constant over time.

Interpretations between multiple mapped paleoshoreline/terrace elevations and predicted sea-level positions are used to produce a correlation among coeval paleoshorelines/terraces along the strike of the Polvica Fault (Figure 10), following similar previous investigations in the Mediterranean realm (e.g., Meschis et al., 2018, 2020, 2022; Roberts et al., 2009, 2013; Robertson et al., 2019, 2023).

Figure 11a,b shows uplift changes with tilted paleoshorelines, suggesting that there is a displacement gradient along the strike of the PF. Considering the Mt. Fellino block, from the west to the east, the elevation of the flight of marine terraces increases up to profile 5 to slightly decrease, as shown by profiles 6 and 7 (Figure 8). Our synchronous correlation unveils that the uplift rate of the PF footwall is constant over the Middle-Late Pleistocene. Yet, the uplift rate changes along the strike of the PF with values of 0.19 mm/yr close to the western fault tip and increases towards the Mt. Fellino ridge centre with an uplift rate of 0.32 mm/yr (Figure 8; Figure 11c). From the centre to the east of Mt. Fellino ridge, the uplift rate slightly decreases to 0.29 mm/yr.

Lacking (i) direct age constraints of the paleoshorelines/terraces and (ii) a well-developed staircase sequence, for Roccarainola hills we tested the two cases abovementioned (i.e., the first case where TRR is coeval with T2 and the second case where TRR coincide with MIS 11. For both cases, the model outputs, using different uplift rates, give comparable R^2 values (close to 1). The first case is supported by an uplift rate of 0.57–0.58 mm/yr (Figure 7), while the second case is supported by an uplift rate of 0.5 mm/yr (Figure 10 and Figure 11c; Table 4). In both cases, an abrupt uplift increase may be inferred for the easternmost footwall block of the PF (Figure 11c).

To investigate whether the along strike tilt angles of the marine terraces imply that the cause of the uplift is associated with normal faulting (e.g., Meschis et al., 2018, 2020, 2022; Roberts et al., 2013; Robertson et al., 2019, 2023), we calculate the tilt angles along strike of the PF from the western tip to the centre. The tilt angle values, which have been calculated according to Meschis et al. (2018), vary between 0.33° to 1°, with the higher and older paleoshorelines/terraces exhibiting higher tilt angles compared to the younger and lower ones (Figure 11d). Such a pattern suggests that progressive faulting through time has caused older paleoshorelines/terraces in the centre of the fault to be tilted at higher angles as a result of the displacement gradients along PF.

Based on the PF uplift reconstruction discussed so far, the throw rate of the PF has been assessed using subsurface data from the T69 borehole. The T69 borehole is located in the Polvica plain approximately aligned with profile 7. A geological cross-section along profile 7 and the T69 borehole has been constructed (Figure 12).

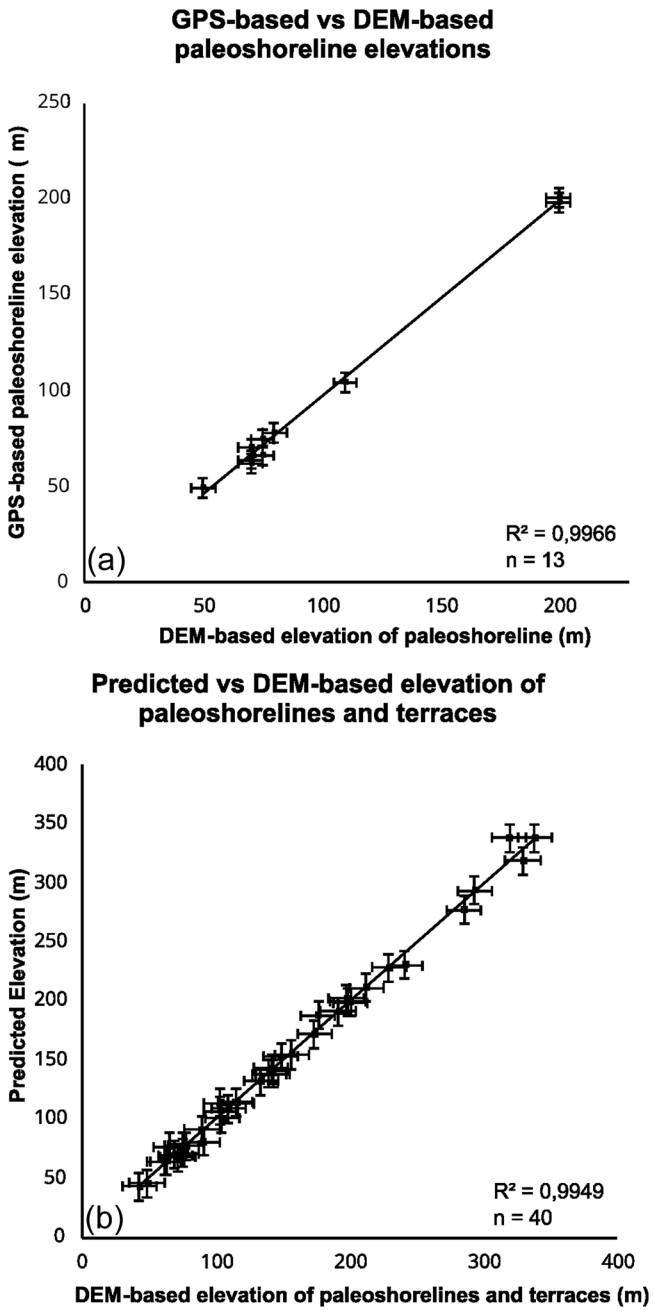

FIGURE 9 (a) Relationship between GPS-based and DEM-based shoreline elevations; (b) relationship between all the measured and predicted paleoshorelines and terraces elevations.

The marine unit b recovered in the T9 borehole (Figure 12) marks the first marine ingression in the hanging wall block of the PF. Assuming that the base of unit b is coeval with the highest and oldest terrace (aged 980 ka by our modelling) identified in the PF footwall, the throw cumulated in the last 980 ka can be estimated from the displacement, measured along profile 7, between the 980 ka terrace and the bottom of marine unit b in T69 borehole. In fact, the top of the limestones in the T69, although with some approximation associated with possible local morphological irregularities, is indicative of the depth of the abrasion platform of unit b ingression.

Based on the above-listed constraints, the inferred mean throw rate for the Mt. Fellino segment of the PF, considering a displacement of 425 m over 980 ka, is 0.43 mm/yr. It is worth noting that the estimated slip rate has been evaluated along a cross-section located, along Mt. Fellino ridge, to the east of the segment and not where the maximum uplift is recorded. This would suggest that the throw rate may be higher if measured in the centre of the fault (i.e., in correspondence of profiles 4–5; Table 1).

5 | DISCUSSION

In this study, as well as worldwide, it has been observed that within zones of plate boundary raised and preserved marine terraces deformed by active faults can be used to estimate rates of crustal deformation spanning the Late Quaternary (e.g., Catalano et al., 2003; Catalano & De Guidi, 2003; De Santis et al., 2023; González-Alfaro et al., 2018; Karymbalis et al., 2022; Malik et al., 2024; Meschis et al., 2022; Ott et al., 2019; Parrino et al., 2022; Roberts et al., 2009, 2013; Robertson et al., 2019; Saillard et al., 2009; Shyu et al., 2018).

In particular, we have constrained the fault-related footwall uplift along the strike of the PF, therefore assessing crustal deformation rates by synchronously correlating multiple uplifted late Quaternary paleoshorelines and terraces.

5.1 | Correlation of paleoshorelines/terraces with Quaternary Sea-level highstands

The terraced surfaces mapped along profiles 1 to 10 include both marine terraces with associated deposits (i.e., paleoshorelines T1, T2 and TRR) and purely erosional terraces (Figure 8). Worthy to note, the predicted sea-level position fits the GPS-measured/DEM-based elevations of the mapped paleoshorelines/terraces (Figures 7 and 9; Section 4.2; Table 3). Such a correspondence supports our uplift reconstruction, consistent with former findings from other areas (e.g., Roberts, 2009).

The starting point for our reconstruction is the presence of two well-preserved paleoshorelines (T1 and T2) along the Mt. Fellino mountain front. Our modelling assumes that the uplift of blocks in the footwall of the PF continues from the late Early Pleistocene until the Present. Holocene activity of the PF is inferred from geomorphic evidence, i.e. the occurrence in the Polvica plain (to the S of the Mt. Fellino ridge) of a topographic low hosting a marshy area, which is consistent with a recent northward tilting/subsidence of the PF hanging wall block (Section 4). This is not unexpected considering that this region has experienced historical earthquakes (Section 1, Figure 1).

Most of the Pleistocene synchronously derived ages of the mapped paleoshorelines/terraces have been identified in the Mediterranean Sea area (e.g., Meschis et al., 2018, 2020, 2022; Roberts et al., 2009, 2013; Robertson et al., 2019, 2023). However, in the PF footwall block, we do not find a geomorphological/stratigraphical record of all the sea-level peaks recorded since 980 ka. We interpret this as the response to multiple reasons. One is the erosion of raised marine terraces in response to sea-cliff retreat during younger highstands (e.g., Cinque, De Pippo, & Romano, 1995), a condition that in our case study is recorded by the landslide deposits that cover the T2 abrasion platform (Cerrone et al., 2021b; Section 2.1). A second reason is the high sedimentation rate in the PF hanging wall block where, besides alluvial deposition, a massive emplacement of pyroclastic/volcanoclastic deposits (c. 70 m thick in the T69 borehole; Section 4) occurred. Abundant deposition of pyroclastic deposits during the late Quaternary (well recorded in the

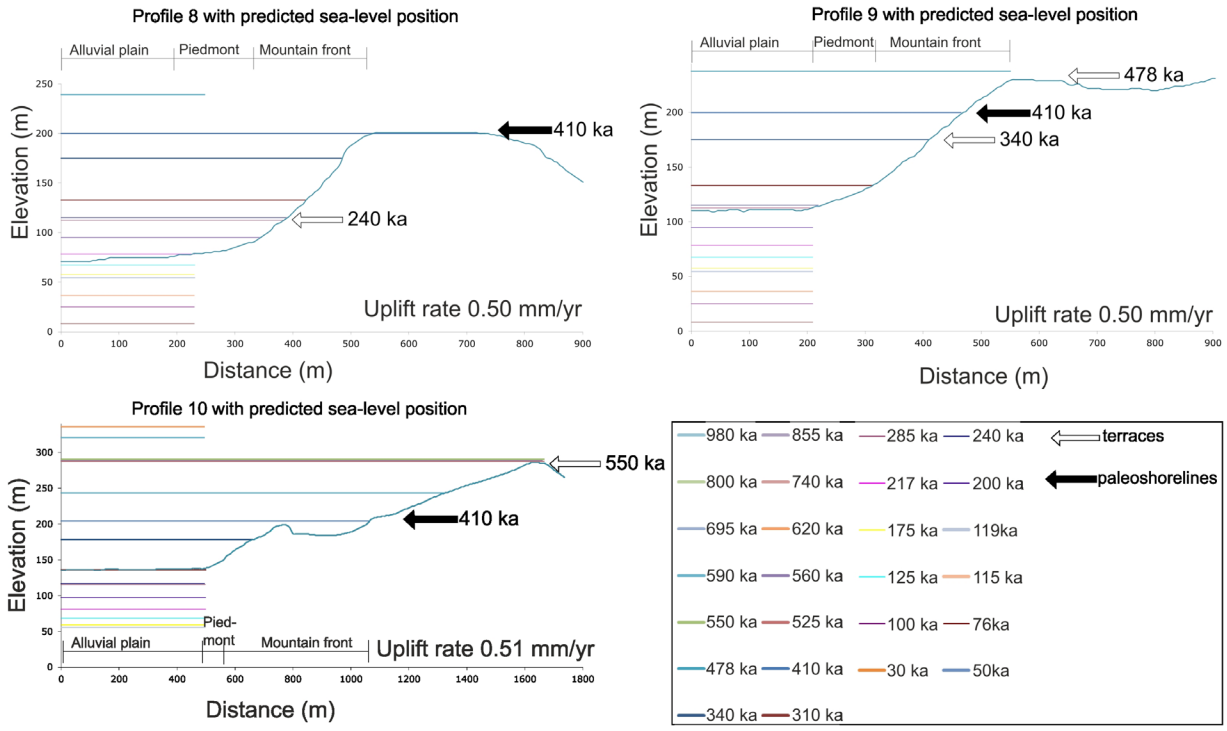

FIGURE 10 Topographic profiles along Roccarainola hills (8 to 10; locations are in Figure 3a). The figure shows the case in which TRR coincides with MIS 11. In the profiles, coloured lines (see the legend for keys to the colours) indicate the sea-level elevations predicted by the modelling; the age of the sea-level peaks are from Siddall et al. (2003) and Rholing et al. (2014) (section 3). The black arrows indicate the positions of the paleoshorelines TRR; the white arrows indicate elevations of the DEM-mapped terraces. Note that there are predicted terraces located below the mountain front-piedmont/alluvial fan junction. The arrows indicate the positions of the mapped terraces with predicted ages.

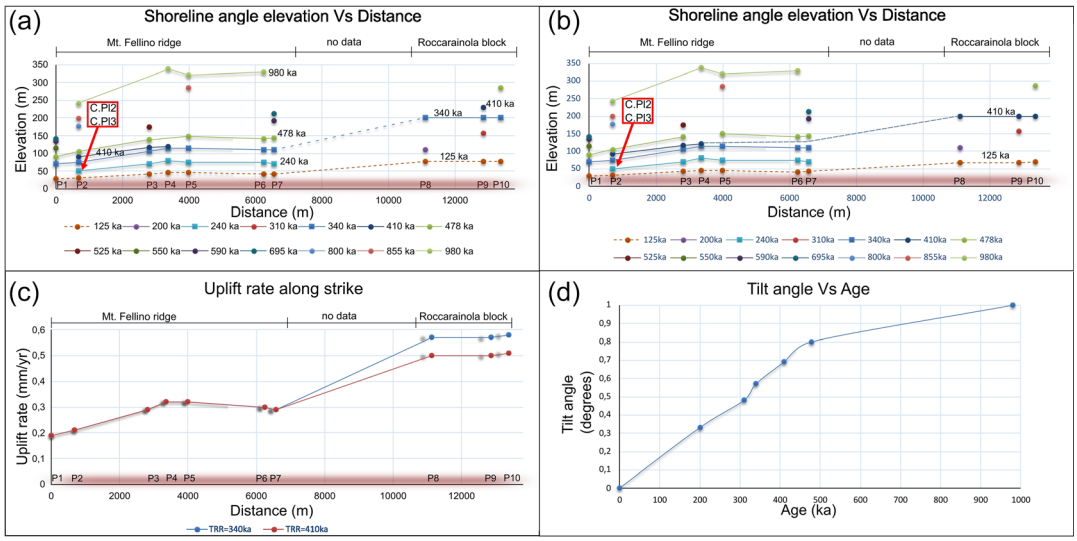

FIGURE 11 Spatial distribution of paleoshorelines/terraces and uplift pattern of the footwall block of the PF. (a) Elevation vs. spatial distribution of the mapped paleoshorelines (squares) and terraces (circles) assuming the case where TRR coincides with T2; the orange dashed line indicates the predicted seal-level position of the MIS 5e, shown for reference. (b) Elevation vs. spatial distribution of the mapped paleoshorelines (squares) and terraces (circles) assuming the case where TRR coincides with MIS 11; the orange dashed line indicates the predicted sea-level position of the MIS 5e, shown for reference. (c) Uplift rate vs. distance along the strike of PF. The uplift rate is lower at the western tip point and higher in the Roccarainola hills. (d) Tilt angles vs. age of the mapped paleoshorelines, showing that the older paleoshorelines, which record a longer history of fault activity, are more tilted than the younger terraces.

entire Campania Plain, e.g., Santangelo et al., 2017) may explain the absence of marine terraces at low predicted elevations. For instance, the Last Interglacial peak (MIS 5e, ~125 ka), if present, would be located at elevations ranging from 29 m, in the west, to 78 m (Figure 11a) or 68 m (Figure 11b), in the east, i.e. systematically below the surface of the Holocene plain or alluvial fans, which also rise eastwards (Section 4.1). A third reason for the lack of distinct geomorphological/stratigraphical records of all the < 980 ka sea level peaks is the overprinting of older by younger marine terraces. The overprinting relies on the interplay between ground vertical motion rate and

TABLE 4 Input data (elevations of paleoshorelines and terraces) and results of the synchronous correlation approach for the Roccarainola block (profiles 8, 9 and 10) based on the assumption that TRR is correlated with MIS 11.

Profile number	Paleoshoreline and terrace label	Latitude (decimal degrees)	Longitude (decimal degrees)	DEM-based elevation of terraces (m)	GPS-based paleoshoreline elevation (m)	Predicted sea level position (m a.s.l.)	Inferred age (ka)
8	1	40.976875°	14.550368°	110	-	115	240
8	4	40.978866°	14.550763°	201	200 (TRR)	200	410
9	3	40.967386°	14.571026°	157	-	175	340
9	4	40.968201°	14.571423°	201	200 (TRR)	200	410
9	5	40.968689°	14.571796°	230	-	239	478
10	4	40.965434°	14.579023°	199	200 (TRR)	204	410
10	6	40.973599°	14.579266°	286	-	291	550

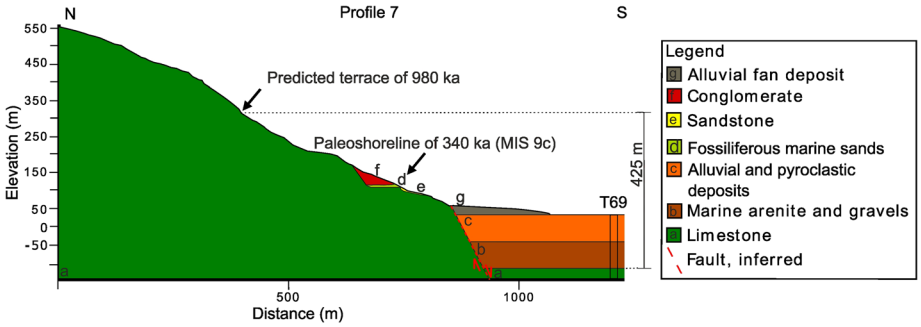

FIGURE 12 Sketch of a geological cross-section along profile 7, where T69 borehole is located (see Figure 9 for location) and its relationship with the higher terrace in the area.

positions of sea levels for past highstands, which were at a variety of paleo elevations above and below present-day sea level (e.g., Cinque, De Pippo, & Romano, 1995; Roberts et al., 2009). Indeed, our interpretation predicts that paleo-shorelines of different ages will, in places, occupy the same elevations, consistent with the findings by Crosetto, de Montserrat, & Oncken (2024). For example, the predicted elevations of the 340 and 410 ka peaks span from 3 to 12 m of each other along Mt. Fellino ridge (profiles 1–7, Figure 7). This limited difference of elevation may explain the rather unique character of the T2 in Mt. Fellino block. Paleoshoreline T2 features markedly horizontal and large size (> 200 m in cross profile) shore platforms (Figure 2) that are suggestive of a poli-phased origin of these platforms and are consistent with their initial formation with the major MIS11 sea level peak and reworking during the 340 ka old MIS 9c.

Profile 2 shows that the predicted 310 ka sea-level highstand is located lower than the 240 ka (Figures 7 and 8). That is a further implication of the interplay between uplift rate and positions of past highstands, which may cause older paleoshorelines to be lower than younger marine terraces. Such a condition, which is not unique to our study area (Cerrone et al., 2021a; De Santis et al., 2023; Pedoja et al., 2018; Roberts et al., 2009), may occur where both moderate uplift rates (Cerrone et al., 2021a) and high uplift rates (Roberts et al., 2009) are recorded, while in tectonic contexts with uplift rates > 0.5–0.6 mm/yr, a well-developed staircase sequence of marine terraces usually is better preserved (Westaway, 1993).

5.2 | Tectonic implications of the Polvica fault activity

The investigated area shows evidence that uplift has varied spatially along the strike of the PF during the Pleistocene. The mapped terraces, including the most continuous paleoshorelines (T1 and T2), occur at different elevations along the mountain fronts underlain by the PF. The uplift rate calculated varies along the strike of the PF from 0.19 to c. 0.3 mm/yr at Mt. Fellino ridge, to rise to 0.5–0.58 mm/yr in the Roccarainola block. The faster uplift of the Roccarainola block is less constrained since a proper staircase of marine terraces along profiles 8–10 is not preserved and independent age constraints are missing. Nonetheless, the correlation of marine terraces all along Mt. Fellino is supported by our modelling, which shows increases in tilt angle values with age (Figure 11d). Such a feature is indicative of fault-controlled crustal deformation, as demonstrated for other areas in the Mediterranean realm influenced by active normal faults (e.g., Armijo et al., 1996; Meschis et al., 2018, 2020, 2022; Roberts et al., 2013; Robertson et al., 2019, 2023). The obtained results have implications in terms of the long-term throw rate of the Mt. Fellino and Roccarainola segments of the PF.

For our study area, it is crucial to recognize that uplifted paleoshorelines have been tectonically deformed with a constant, but spatially variable (Figure 11a,b), rate through time suggesting that the PF throw rates are constant over the Late Quaternary, with important implications for the seismic hazard of the region and the broader tectonic effects. Indeed, results from this study have allowed us to derive a refined throw rate across the PF. The obtained value, which is lower than values estimated for the PF in both the short and long-term by Cinque et al. (2000), permits an assessment of the relative importance of the PF if compared to other faults within the Italian territory in terms of seismic hazard. A throw rate of 0.43 mm/yr is in the range of 0.3–2.34 mm/yr values estimated for other active faults in the Italian Territory such as in Central Apennines and the Calabrian-Peloritani forearc (e.g., Faure Walker et al., 2012; Lavecchia et al., 2024; Roberts & Michetti, 2004; Sgambato et al., 2023). From this, it is also important to highlight that to produce a throw rate of 0.43 mm/yr

given ~600-mm maximum vertical slip events in Mw ~ 6.2 earthquakes, assuming a coseismic rupture of the entire fault length of PF considered in this study, implies an ERI value (or T_{mean}) of 1,250 yr. This value is similar to those measured from active normal faults within the Italian Territory by historical records, palaeoseismological and displaced marine terraces investigations (e.g., Galli, Galadini, & Pantosti, 2008; Lavecchia et al., 2024; Meschis et al., 2022; Roberts et al., 2013). Worth noting that for the PF we considered a length of ~ 15 km, from the western part of Mt. Fellino ridge, to the Roccarainola hills, where we mapped raised marine terraces, but, the PF might continue on both sides, hence our results may be considered as minimum values. However, more detailed investigations are needed to assess the palaeoseismological history of the PF.

Turning the results from this work to the broader tectonic framework for the southern Apennines, it is important to highlight if the PF should be considered an active fault, however, the link between the PF activity and volcanic hazard from historical Vesuvius eruptions is understudied. For instance, it has been suggested a mutual coupling between the nucleation of earthquakes in the southern Apennines and eruptions from Vesuvius (Nostro et al., 1998). Indeed, by Coulomb Stress Change investigations elastic stress interaction between earthquakes and eruptions has been proved within the Mt. Vesuvius region in the Southern Apennines as well as the Mt. Etna region in Sicily (southern Italy; Feuillet et al., 2006). Note that the PF is bounding the Campania Plain where the Mt. Vesuvius volcanic complex lies within a distance of ~ 15 km. This should lead to a reappraising of the long-term seismic-volcano hazard taking into account the faulting activity of the PF since the Middle Pleistocene, also because the PF may produce seismic events with M > 6, which are "missing" within the Italian historical Catalogue of Earthquakes.

This work stresses that more investigations are needed for the future where the interaction between Quaternary faulting activity, historical volcanic activity and their stress interaction takes into account new knowledge and results provided in this work.

6 | CONCLUSIONS

In this work, a constant uplift rate on the Polvica extensional fault system from the late Early Pleistocene onward has been reconstructed by analysis and modelling with the synchronous correlation method of the raised paleoshorelines and terraces along the Mt. Fellino ridge and Roccarainola hills. This modelling has been deformed by the PF, constrained by U-series age on calcite veins into the marine deposits associated with the T2 paleoshorelines (MIS 9c, 340 ka). The work shows how the PF zone has moved and raised the paleoshorelines and terraces on the Mt. Fellino ridge at least from the late Early Pleistocene and geomorphological evidence indicates that the PF was active during the late Quaternary. The slip rate varies along the strike of the PF and in particular it is lower (0.19 mm/yr) at the western tip and increases eastward to 0.50–0.58 mm/yr. PF has folded and tilted the analysed paleoshorelines and it is clear that the lower, and younger, paleoshorelines have experienced a shorter deformation history.

Historical seismic activity of the PF is still not known, however, the magnitude and slip rate estimated with our work raises the crucial question of a careful assessment of seismic hazard for the Campania Plain, where several towns are settled. The constant throw rate calculated by integration of surface and subsurface data from the Middle Pleistocene is of ca. 0.4 mm/yr, and the Tmean calculated if the entire 15 km, from the western termination of Mt. Fellino to Roccarainola hills, of PF will displace at the same time, is 1,250 yr. Although some assumptions and uncertainties affect our estimates of possible earthquake ruptures, based on our results on late Quaternary activity of the PF zone further, more in-depth analyses addressing reassessment of the seismic hazard for the densely populated Campania Plain are strongly recommended.

AUTHOR CONTRIBUTIONS

All authors have contributed substantially to the manuscript, reviewed and edited the final version and approved the submitted manuscript. In particular, C.C. wrote the original draft; C.C., G.P.R., J.R. and M.M. conceived the study; C. C and A.A. conducted the fieldwork, carried out the core of the geomorphological study and interpretation of the stratigraphic cores; C.C. prepared the sample and cooperated on the U-series analyses; P.T. and M.S. carried out and supervised the geochronological analyses.

ACKNOWLEDGEMENTS

The authors acknowledge PALSEA, a working group of the International Union for Quaternary Sciences (INQUA) and Past Global Changes (PAGES), which in turn received support from the Swiss Academy of Sciences and the Chinese Academy of Sciences. This paper also gained valuable insights from the discussions during the meetings of the AIGeo (Associazione Italiana di Geografia Fisica e Geomorfologia) Working Group on 'SIStemi e TECnologie integrati per l'analisi morfoTettonica' (SISTECT).

We want to thank the two anonymous reviewers whose suggestions significantly improved the manuscript. Open access publishing facilitated by Universita Ca' Foscari, as part of the Wiley - CRUI-CARE agreement.

CONFLICT OF INTEREST STATEMENT

The authors declare that they have no known competing financial interests or personal relationships that could have appeared to influence the work reported in this paper. C.C. declares that he is the Guest Editor of the Special Issue "*The Geomorphic Signature of Marine and Continental Quaternary Deposits*", but that this did not affect the reviewing process.

ORCID

Ciro Cerrone https://orcid.org/0000-0001-8503-2658
Marco Meschis https://orcid.org/0000-0001-9144-3031
Jennifer Robertson https://orcid.org/0000-0002-0849-6050

REFERENCES

Aiello, G., Amato, V., Aucelli, P.P.C., Barra, D., Corrado, G., Di Leo, P., et al. (2021) Multiproxy study of cores from the Garigliano plain: an insight into the Late Quaternary coastal evolution of central-southern Italy. *Palaeogeography Palaeoclimatology Palaeoecology*, 567, 110298. Available from: https://doi.org/10.1016/j.palaeo.2021.110298

Amorosi, A., Pacifico, A., Rossi, V. & Ruberti, D. (2012) Late Quaternary incision and deposition in an active volcanic setting: the Volturno valley fill, southern Italy. *Sedimentary Geology*, 282, 307–320. Available from: https://doi.org/10.1016/j.sedgeo.2012.10.003

Aprile, F., Sbrana, A. & Toccaceli, R.M. (2004) Dei Terreni Quaternari Del Sottosuolo Della Piana Campana (Italia Meridionale). *Il Quaternario - Italian Journal of Quaternary Sciences*, 17(2/1), 547–554.

Armijo, R., Meyer, B., King, G.C.P., Rigo, A. & Papanastassiou, D. (1996) Summary for policymakers, in: intergovernmental panel on climate change. In: *Climate change 2013 - the physical science basis*. Cambridge: Cambridge University Press, pp. 1–30 https://doi.org/10.1017/CBO9781107415324.004

Barra, D., Cinque, A., Gewelt, M. & Hurtgen, C. (1991) L'ospite caldo Sylvestra seminis (Bonaduce, Masoli & Pugliese, 1976) (Crustacea, Ostracoda): un possibile marker dell'Ultimo Interglaciale dell'area Mediterranea. *Il Quaternario*, 4(2), 327–332.

Barra, D., Romano, P., Santo, A., Campajola, L., Roca, V. & Tuniz, C. (1996) The Versilian trasgression in the Volturno river plain (Campania, southern Italy): palaeoenvironmental history and chronological data. *Il Quaternario*, 9, 445–458.

Bellucci, F., Santangelo, N. & Santo, A. (2003) Segnalazione di nuovi depositi piroclastici intercalati alle successioni continentali Pleistocene superiore-Olocene dela porzione nord-orientale della Piana Campana. *Italian Journal of Quaternary Sciences*, 16(2), 279–287.

Brancaccio, L., Cinque, A., Romano, P., Rosskopf, C., Russo, F. & Santangelo, N. (1995) L'evoluzione delle pianure costiere della Campania: Geomorfologia e Neotettonica. *Mem. Soc. Geogr. Ital.*, LIII, 313–337.

Brancaccio, L., Cinque, A., Romano, P., Rosskopf, C., Russo, F., Santangelo, N., et al. (1991) Geomorphology and neotectonic evolution of a sector of the Tyrrhenian flank of the southern Apennines (region of Naples, Italy). *Zeitschrift für Geomorphologie N.F*, 82, 47–58.

Bruno, P.P.G., Cippitelli, G. & Rapolla, A. (1998) Seismic study of the Mesozoic carbonate basement around Mt. Somma–Vesuvius, Italy. *Journal of Volcanology and Geothermal Research*, 84, 311–322. Available from: https://doi.org/10.1016/S0377-0273(98)00023-7

Caiazzo, C., Ascione, A. & Cinque, A. (2006) Late tertiary-quaternary tectonics of the southern Apennines (Italy): new evidences from the Tyrrhenian slope. *Tectonophysics*, 421(1-2), 23–51. Available from: https://doi.org/10.1016/j.tecto.2006.04.011

Catalano, S. & De Guidi, G. (2003) Late Quaternary uplift of northeastern Sicily: relation with the active normal faulting deformation. *Journal of Geodynamics*, 36(4), 445–467. Available from: https://doi.org/10.1016/S0264-3707(02)00035-2

Catalano, S., De Guidi, G., Monaco, C., Tortorici, G. & Tortorici, L. (2003) Long-term behaviour of the late Quaternary normal faults in the straits of Messina area (Calabria arc): structural and morphological constraints. *Quaternary International*, 101(102), 81–91. Available from: https://doi.org/10.1016/S1040-6182(02)00091-5

Cella, F., Fedi, M., Florio, G., Grimaldi, M. & Rapolla, A. (2007) Shallow structure of the Somma-Vesuvius volcano from 3D inversion of gravity data. *Journal of Volcanology and Geothermal Research*, 161(4), 303–317. Available from: https://doi.org/10.1016/j.jvolgeores.2006.12.013

Cerrone, C., Ascione, A., Robustelli, G., Tuccimei, P., Soligo, M., Balassone, G., et al. (2021a) Late Quaternary uplift and sea level fluctuations along the Tyrrhenian margin of Basilicata - northern Calabria (southern Italy): new constraints from raised paleoshorelines. *Geomorphology*, 395, 107978. Available from: https://doi.org/10.1016/j.geomorph.2021.107978

Cerrone, C., Di Donato, V., Mazzoli, S., Robustelli, G., Soligo, M., Tuccimei, P., et al. (2021b) Development and deformation of marine terraces: constraints to the evolution of the Campania plain quaternary coastal basin (Italy). *Geomorphology*, 385, 107725. Available from: https://doi.org/10.1016/j.geomorph.2021.107725

Cerrone, C., Vacchi, M., Fontana, A. & Rovere, A. (2021c) Last interglacial sea-level proxies in the western Mediterranean. *Earth System Science Data*, 13(9), 4485–4527. Available from: https://doi.org/10.5194/essd-13-4485-2021

Chauveau, D., Authemayou, C., Pedoja, K., Molliex, S., Husson, L., Scholz, D., et al. (2021) On the generation and degradation of emerged coral reef terrace sequences: first cosmogenic 36Cl analysis at cape Laundi, Sumba Island (Indonesia). *Quaternary Science Reviews*, 269, 107144. Available from: https://doi.org/10.1016/j.quascirev.2021.107144

Chauveau, D., Georgiou, N., Cerrone, C., Dean, S. & Rovere, A. (2024) Sea-level oscillations within the last interglacial: insights from coral reef stratigraphic forward modelling. *Quaternary Science Reviews*, 336, 108759. Available from: https://doi.org/10.1016/j.quascirev.2024.108759

Cinque, A. (1991) La trasgressione versiliana nella piana del Sarno (Campania). *Geografia Fisica e Dinamica Quaternaria*, 14, 63–71.

Cinque, A., Ascione, A. & Caiazzo, C. (2000) Spatial and temporal distribution of Quaternary faulting in the Southern Apennines. In: Galadini, F., Meletti, C. & Rebez, A. (Eds.) *Le ricerche del GNDT nel campo della pericolosità sismica*. Roma (In Italian with English abstract): CNR- Gruppo Nazionale per la difesa dai Terremoti.

Cinque, A., De Pippo, T. & Romano, P. (1995) Coastal slope terracing and relative sea-level changes: deductions based on computer simulations. *Earth Surface Processes and Landforms*, 20(1), 87–103. Available from: https://doi.org/10.1002/esp.3290200108

Corrado, G., Amodio, S., Aucelli, P. P. C., Gioia, D., Pappone, G., & Schiattarella, M. (2024). Reconstructing active tectonics from land–sea correlations based on cross-interpretation of core and seismic data for the Tyrrhenian coastal segment in southern Italy. *Earth Surface Processes and Landforms*. https://doi.org/10.1002/esp.6049

Corrado, G., Amodio, S., Aucelli, P.P.C., Pappone, G. & Schiattarella, M. (2020) The subsurface geology and landscape evolution of the Volturno coastal plain, Italy: interplay between tectonics and sea-level changes during the quaternary. *Water (Switzerland)*, 12(12), 3386. Available from: https://doi.org/10.3390/w12123386

Crosetto, S., de Montserrat, A. & Oncken, O. (2024) Uplifted Pleistocene marine terraces at active margins: modeling reveals the effects of sea reoccupation and coseismic uplift on uplift rate calculation. *Geochemistry, Geophysics, Geosystems*, 25(4), e2023GC011036. Available from: https://doi.org/10.1029/2023GC011036

De Gelder, G., Fernández-Blanco, D., Öğretmen, N., Liakopoulos, S., Papanastassiou, D., Faranda, C., et al. (2022) Quaternary E-W extension uplifts Kythira Island and segments the Hellenic Arc. *Tectonics*, 41(10), e2022TC007231. Available from: https://doi.org/10.1029/2022TC007231

De Santis, V., Scardino, G., Scicchitano, G., Meschis, M., Montagna, P., Pons-Branchu, E., et al. (2023) Middle-late Pleistocene chronology of palaeoshorelines and uplift history in the low-rising to stable Apulian foreland: overprinting and reoccupation. *Geomorphology*, 421, 108530. Available from: https://doi.org/10.1016/j.geomorph.2022.108530

Decker, V., Falkenroth, M. & Hoffmann, G. (2024) Sedimentological evidence of Late Pleistocene shorelines in Oman. *Marine Geology*, 477, 107407. Available from: https://doi.org/10.1016/j.margeo.2024.107407

Devoti, R., D'Agostino, N., Serpelloni, E., Pietrantonio, G., Riguzzi, F., Avallone, A., et al. (2017) A combined velocity field of the Mediterranean region. *Annals of Geophysics*, 60(2), S0215. Available from: https://doi.org/10.4401/ag-7059

DISS Working group, 2018. *Database of individual seismogenic sources (DISS), version 3.2.1*. Istituto Nazionale di Geofisica e Vulcanologia (INGV). https://doi.org/10.6092/INGV.IT-DISS3.2.1

Faure Walker, J.P., Roberts, G.P., Cowie, P.A., Papanikolaou, I., Michetti, A.M., Sammonds, P., et al. (2012) Relationship between topography, rates of extension and mantle dynamics in the actively-extending Italian Apennines. *Earth and Planetary Science Letters*, 325–326, 76–84. Available from: https://doi.org/10.1016/j.epsl.2012.01.028

Ferranti, L. & Oldow, J.S. (2005) Latest Miocene to quaternary horizontal and vertical displacement rates during simultaneous contraction and extension in the southern Apennines orogen, Italy. *Terra Nova*, 17(3), 209–214. Available from: https://doi.org/10.1111/j.1365-3121.2005.00593.x

Feuillet, N., Cocco, M., Musumeci, C. & Nostro, C. (2006) Stress interaction between seismic and volcanic activity at Mt Etna. *Geophysical Journal*

International, 164(3), 697–718. Available from: https://doi.org/10.1111/j.1365-246X.2005.02824.x

Florio, G., Fedi, M., Cella, F. & Rapolla, A. (1999) The Campanian plain and Phlegrean fields: structural setting from potential field data. *Journal of Volcanology and Geothermal Research*, 91(2-4), 361–379. Available from: https://doi.org/10.1016/S0377-0273(99)00044-X

Galli, P., Galadini, F. & Pantosti, D. (2008) Twenty years of paleoseismology in Italy. *Earth-Science Reviews*, 88(1-2), 89–117. Available from: https://doi.org/10.1016/j.earscirev.2008.01.001

Georgiou, N., Geraga, M., Francis-Allouche, M., Christodoulou, D., Stocchi, P., Fakiris, E., et al. (2022) Late Pleistocene submarine terraces in the eastern Mediterranean, Central Lebanon, Byblos: revealing their formation time frame through modeling. *Quaternary International*, 638–639, 180–196. Available from: https://doi.org/10.1016/j.quaint.2021.12.008

Giaccio, B., Hajdas, I., Isaia, R., Deino, A. & Nomade, S. (2017) High-precision 14C and 40Ar/39Ar dating of the Campanian ignimbrite (Y-5) reconciles the time-scales of climatic-cultural processes at 40 ka. *Scientific Reports*, 7(1), 45940. Available from: https://doi.org/10.1038/srep45940

González-Alfaro, J., Vargas, G., Ortlieb, L., González, G., Ruiz, S., Báez, J.C., et al. (2018) Abrupt increase in the coastal uplift and earthquake rate since ~40 ka at the northern Chile seismic gap in the Central Andes. *Earth and Planetary Science Letters*, 502, 32–45. Available from: https://doi.org/10.1016/j.epsl.2018.08.043

Houghton, S.L., Roberts, G.P., Papanikolaou, I.D. & McArthur, J.M. (2003) New 234 U- 230 Th coral dates from the western gulf of Corinth: implications for extensional tectonics. *Geophysical Research Letters*, 30(19), 2013. Available from: https://doi.org/10.1029/2003GL018112

Ippolito, F., Ortolani, F. & Russo, M. (1973) Struttura marginale tirrenica dell'Appennino Campano: Reiterpretazione di dati di antiche ricerche di idrocarburi. *Memorie Della Societa Geologica Italiana*, 12, 227–250.

ITHACA Working Group, 2019. ITHACA (ITaly HAzard from CApable faulting), A database of active capable faults of the Italian territory. Version December 2019.ISPRA Geological Survey of Italy. Web Portal http://sgi2.isprambiente.it/ithacaweb/Mappatura.aspx

Karymbalis, E., Tsanakas, K., Tsodoulos, I., Gaki-Papanastassiou, K., Papanastassiou, D., Batzakis, D.-V., et al. (2022) Late Quaternary marine terraces and tectonic uplift rates of the broader Neapolis area (SE Peloponnese, Greece). *Journal of Marine Science and Engineering*, 2022(10), 99. Available from: https://doi.org/10.3390/jmse10010099

Lajoie, K. (1986) Coastal tectonics. *Active Tectonics*. National Academy Press: Washington, DC, pp. 95–124.

Lavecchia, G., Bello, S., Andrenacci, C., Cirillo, D., Pietrolungo, F., Talone, D., et al. (2024) QUIN 2.0 - new release of the QUaternary fault strain INdicators database from the southern Apennines of Italy. *Scientific Data*, 11(1), 189. Available from: https://doi.org/10.1038/s41597-024-03008-6

Li, H., You, D., Han, J., Qian, Y., Sha, X. & Xi, B. (2020) The origin of fluid in calcite veins and its implications for hydrocarbon accumulation in the Shunnan-Gucheng area of the Tarim Basin, China. *Journal of Natural Gas Geoscience*, 5(6), 341–353. Available from: https://doi.org/10.1016/j.jnggs.2020.11.001

Ludwing, K.R. (2003) *User's Manual for Isoplot/Ex, Version 3.00. A Geochronological Toolkit for Microsoft Excel*. Berkeley Geochronology Center Special Publication, 4(2), 1–70.

Malik, J. N., Srivastava, E., Gadhavi, M. S., Livio, F., Sharma, N., Arora, S., Parrino, N., Burrato, P., & Sulli, A. (2024). Holocene surface-rupturing paleo-earthquakes along the Kachchh Mainland Fault: shaping the seismic landscape of Kachchh, Western India. *Scientific Reports*, 14(1), 11612. https://doi.org/10.1038/s41598-024-62086-z

Mariani, M., Prato, R., 1988. I bacini neogenici costieri del margine tirrenico: Approccio sismico-stratigrafico. *Memorie della Società Geologica Italiana*, 41, 519-531.

Meschis, M., Roberts, G.P., Robertson, J. & Briant, R.M. (2018) The relationships between regional quaternary uplift, deformation across active Normal faults, and historical seismicity in the upper plate of subduction zones: the capo D'Orlando fault, NE Sicily. *Tectonics*, 37(5), 1231–1255. Available from: https://doi.org/10.1029/2017TC004705

Meschis, M., Roberts, G.P., Robertson, J., Mildon, Z.K., Sahy, D., Goswami, R., et al. (2022) Out of phase quaternary uplift-rate changes reveal normal fault interaction, implied by deformed marine palaeoshorelines. *Geomorphology*, 416, 108432. Available from: https://doi.org/10.1016/j.geomorph.2022.108432

Meschis, M., Scicchitano, G., Roberts, G.P., Robertson, J., Barreca, G., Monaco, C., et al. (2020) Regional deformation and offshore crustal local faulting as combined processes to explain uplift through time constrained by investigating differentially uplifted Late Quaternary Paleoshorelines: the foreland Hyblean plateau, SE Sicily. *Tectonics*, 39(12), e2020TC006187. Available from: https://doi.org/10.1029/2020tc006187

Milia, A. & Torrente, M.M. (1999) Tectonics and stratigraphic architecture of a peri-Tyrrhenian half-graben (bay of Naples, Italy). *Tectonophysics*, 315(1-4), 301–318. Available from: https://doi.org/10.1016/S0040-1951(99)00280-2

Milia, A. & Torrente, M.M. (2015) Tectono-stratigraphic signature of a rapid multistage subsiding rift basin in the Tyrrhenian-Apennine hinge zone (Italy): a possible interaction of upper plate with subducting slab. *Journal of Geodynamics*, 86, 42–60. Available from: https://doi.org/10.1016/j.jog.2015.02.005

Milia, A., Torrente, M.M., Massa, B. & Iannace, P. (2013) Progressive changes in rifting directions in the Campania margin (Italy): new constrains for the Tyrrhenian Sea opening. *Glob Planet Change*, 109, 3–17. Available from: https://doi.org/10.1016/j.gloplacha.2013.07.003

Nostro, C., Stein, R.S., Cocco, M., Belardinelli, M.E. & Marzocchi, W. (1998) Two-way coupling between Vesuvius eruptions and southern Apennine earthquakes, Italy, by elastic stress transfer. *Journal of Geophysical Research: Solid Earth*, 103(B10), 24487–24504. Available from: https://doi.org/10.1029/98JB00902

Ott, R.F., Gallen, S.F., Wegmann, K.W., Biswas, R.H., Herman, F. & Willett, S.D. (2019) Pleistocene terrace formation, quaternary rock uplift rates and geodynamics of the Hellenic subduction zone revealed from dating of paleoshorelines on Crete, Greece. *Earth and Planetary Science Letters*, 525, 115757. Available from: https://doi.org/10.1016/j.epsl.2019.115757

Palano, M., Cannavò, F., Ferranti, L., Mattia, M. & Mazzella, M.E. (2011) Strain and stress fields in the southern Apennines (Italy) constrained by geodetic, seismological and borehole data. *Geophysical Journal International*, 187(3), 1270–1282. Available from: https://doi.org/10.1111/j.1365-246X.2011.05234.x

Papanikolaou, I.D. & Roberts, G.P. (2007) Geometry, kinematics and deformation rates along the active normal fault system in the southern Apennines: implications for fault growth. *Journal of Structural Geology*, 29(1), 166–188. Available from: https://doi.org/10.1016/j.jsg.2006.07.009

Parrino, N., Burrato, P., Sulli, A., Gasparo Morticelli, M., Agate, M., Srivastava, E., Malik, J. N., & Di Maggio, C. (2023). Plio-Quaternary coastal landscape evolution of north-western Sicily (Italy). *Journal of Maps*, 19(1), 2159889. https://doi.org/10.1080/17445647.2022.2159889

Parrino, N., Pepe, F., Burrato, P., Dardanelli, G., Corradino, M., Pipitone, C., Morticelli, M. G., Sulli, A., & Di Maggio, C. (2022). Elusive active faults in a low strain rate region (Sicily, Italy): Hints from a multidisciplinary land-to-sea approach. *Tectonophysics*, 839, 229520. https://doi.org/10.1016/j.tecto.2022.229520

Pedoja, K., Jara-Muñoz, J., De Gelder, G., Robertson, J., Meschis, M., Fernandez-Blanco, D., et al. (2018) Neogene-quaternary slow coastal uplift of Western Europe through the perspective of sequences of strandlines from the Cotentin peninsula (Normandy, France). *Geomorphology*, 303, 338–356. Available from: https://doi.org/10.1016/j.geomorph.2017.11.021

Perazzotti, F., Del Valle, L. & Fornós, J.J. (2024a) Upper Pleistocene in Mallorca: sedimentary variability of littoral units in relation to different structural contexts. *Quaternary International*, 709, 1–14. Available from: https://doi.org/10.1016/j.quaint.2024.08.005

Perazzotti, F., Del Valle, L. & Fornós, J.J. (2024b) An overview of Upper Pleistocene coastal deposits on Mallorca island. *Quaternary International*, 707, 60–71.

Roberts, G.P., Houghton, S.L., Underwood, C., Papanikolaou, I., Cowie, P.A., van Calsteren, P., et al. (2009) Localization of quaternary slip rates in an active rift in 10 5 years: an example from Central Greece constrained by 234 U- 230 Th coral dates from uplifted paleoshorelines. *Journal of Geophysical Research*, 114(B10), B10406. Available from: https://doi.org/10.1029/2008JB005818

Roberts, G.P., Meschis, M., Houghton, S., Underwood, C. & Briant, R.M. (2013) The implications of revised quaternary palaeoshoreline chronologies for the rates of active extension and uplift in the upper plate of subduction zones. *Quaternary Science Reviews*, 78, 169–187. Available from: https://doi.org/10.1016/j.quascirev.2013.08.006

Roberts, G.P. & Michetti, A.M. (2004) Spatial and temporal variations in growth rates along active normal fault systems: an example from the Lazio-Abruzzo Apennines, Central Italy. *Journal of Structural Geology*, 26(2), 339–376. Available from: https://doi.org/10.1016/S0191-8141(03)00103-2

Robertson, J., Meschis, M., Roberts, G.P., Ganas, A. & Gheorghiu, D.M. (2019) Temporally constant quaternary uplift rates and their relationship with extensional upper-plate faults in South Crete (Greece), constrained with 36Cl cosmogenic exposure dating. *Tectonics*, 38(4), 1189–1222. Available from: https://doi.org/10.1029/2018TC005410

Robertson, J., Roberts, G.P., Ganas, A., Meschis, M., Gheorghiu, D.M. & Shanks, R.P. (2023) Quaternary uplift of palaeoshorelines in southwestern Crete: the combined effect of extensional and compressional faulting. *Quaternary Science Reviews*, 316, 108240. Available from: https://doi.org/10.1016/j.quascirev.2023.108240

Rohling, E. J., Foster, G. L., Grant, K. M., Marino, G., Roberts, A. P., Tamisiea, M. E., & Williams, F. (2014). Sea-level and deep-sea-temperature variability over the past 5.3 million years. *Nature*, 508(7497), 477–482. https://doi.org/10.1038/nature13230

Romano, P., Santo, A. & Voltaggio, M. (1994) L'evoluzione geomorfologica della piana del fiume Volturno (Campania) durante il tardo Quaternario (Pleistocene medio-superiore-Olocene). *Il Quaternario - Italian Journal of Quaternary Sciences, 7(1/a), 41-56.*

Rovida, A., Locati, M., Camassi, R., Lolli, B. & Gasperini, P. (2020) The Italian earthquake catalogue CPTI15. *Bulletin of Earthquake Engineering*, 18(7), 2953–2984. Available from: https://doi.org/10.1007/s10518-020-00818-y

Rovida, A., Locati, M., Camassi, R., Lolli, B., Gasperini, P., Antonucci, A., 2021. *Catalogo Parametrico dei Terremoti Italiani (CPTI15), versione 3.0*. Istituto Nazionale di Geofisica e Vulcanologia. https://doi.org/10.13127/CPTI/CPTI15.3

Rubio-Sandoval, K., Rovere, A., Cerrone, C., Stocchi, P., Lorscheid, T., Felis, T., et al. (2021) A review of last interglacial sea-level proxies in the western Atlantic and southwestern Caribbean, from Brazil to Honduras. *Earth System Science Data*, 13(10), 4819–4845. Available from: https://doi.org/10.5194/essd-13-4819-2021

Rubio-Sandoval, K., Ryan, D.D., Richiano, S., Giachetti, L.M., Hollyday, A., Bright, J., et al. (2024) Quaternary and Pliocene sea-level changes at Camarones, Central Patagonia, Argentina. *Quaternary Science Reviews*, 345, 108999. Available from: https://doi.org/10.1016/j.quascirev.2024.108999

Saillard, M., Hall, S.R., Audin, L., Farber, D.L., Hérail, G., Martinod, J., et al. (2009) Non-steady long-term uplift rates and Pleistocene marine terrace development along the Andean margin of Chile (31°S) inferred from 10Be dating. *Earth and Planetary Science Letters*, 277(1-2), 50–63. Available from: https://doi.org/10.1016/j.epsl.2008.09.039

Santangelo, N., Ciampo, G., Di Donato, V., Esposito, P., Petrosino, P., Romano, P., et al. (2010) Late quaternary buried lagoons in the northern Campania plain (southern Italy): evolution of a coastal system under the influence of volcano-tectonics and eustatism. *Italian Journal of Geosciences*, 129(1), 156–175. Available from: https://doi.org/10.3301/IJG.2009.12

Santangelo, N., Romano, P., Ascione, A. & Russo Ermolli, E. (2017) Quaternary evolution of the southern Apennines coastal plains: a review. *Geologica Carpathica*, 68(1), 43–56. Available from: https://doi.org/10.1515/geoca-2017-0004

Santo, A., Santangelo, N., De Falco, M., Forte, G. & Valente, E. (2019) Cover collapse sinkhole over a deep buried carbonate bedrock: the case study of Fossa san Vito (Sarno - southern Italy). *Geomorphology*, 345, 106838. Available from: https://doi.org/10.1016/j.geomorph.2019.106838

Sartori, R. (1990) The Main results of ODP leg 107 in the frame of Neogene to recent geology of Peri-Tyrrhenian areas. *Proceedings of the Ocean Drilling Program, Scientific Results*, 107(107), 715–730. Available from: https://doi.org/10.2973/odp.proc.sr.107.183.1990

Scandone, R., Bellucci, F., Lirer, L. & Rolandi, G. (1991) The structure of the Campanian plain and the activity of the Neapolitan volcanoes (Italy). *Journal of Volcanology and Geothermal Research*, 48(1-2), 1–31. Available from: https://doi.org/10.1016/0377-0273(91)90030-4

Scarpati, C., Chiominto, G., Santangelo, I., Perrotta, A. & Fedele, L. (2025a) The 79 AD Vesuvius eruption revisited: Plinian and post-Plinian falls. *Journal of the Geological Society of London*, 182(1), Available from: https://doi.org/10.1144/jgs2024-071

Scarpati, C., Santangelo, I., Chiominto, G., Perrotta, A., Branney, M.J. & Fedele, L. (2025b) The 79 AD Vesuvius eruption revisited: the pyroclastic density currents. *Journal of the Geological Society of London*, 182(1), Available from: https://doi.org/10.1144/jgs2024-072

Serpelloni, E., Anzidei, M., Baldi, P., Casula, G. & Galvani, A. (2005) Crustal velocity and strain-rate fields in Italy and surrounding regions: new results from the analysis of permanent and non-permanent GPS networks. In. *Geophysical Journal International*, 161(3), 861–880. Available from: https://doi.org/10.1111/j.1365-246X.2005.02618.x

Serpelloni, E., Cavaliere, A., Martelli, L., Pintori, F., Anderlini, L., Borghi, A., et al. (2022) Surface velocities and strain-rates in the Euro-Mediterranean region from massive GPS data processing. *Frontiers in Earth Science*, 10, 907897. Available from: https://doi.org/10.3389/feart.2022.907897

Sgambato, C., Faure Walker, J.P. & Roberts, G.P. (2020) Uncertainty in strain-rate from field measurements of the geometry, rates and kinematics of active normal faults: implications for seismic hazard assessment. *Journal of Structural Geology*, 131, 103934. Available from: https://doi.org/10.1016/j.jsg.2019.103934

Sgambato, C., Faure, W.J.P., Roberts, G.P., Mildon, Z.K. & Meschis, M. (2023) Influence of fault system geometry and slip rates on the relative role of coseismic and interseismic stresses on earthquake triggering and recurrence variability. *Journal of Geophysical Research: Solid Earth*, 128(11), e2023JB02496. Available from: https://doi.org/10.1029/2023JB026496

Shyu, J.B.H., Wang, C.C., Wang, Y., Shen, C.C., Chiang, H.W., Liu, S.C., et al. (2018) Upper-plate splay fault earthquakes along the Arakan subduction belt recorded by uplifted coral microatolls on northern Ramree Island, western Myanmar (Burma). *Earth and Planetary Science Letters*, 484, 241–252. Available from: https://doi.org/10.1016/j.epsl.2017.12.033

Siddall, M., Rohling, E.J., Almogi-Labin, A., Hemleben, C., Meischner, D., Schmelzer, I., et al. (2003) Sea-level fluctuations during the last glacial cycle. *Nature*, 423(6942), 853–858. Available from: https://doi.org/10.1038/nature01690

Sorrentino, A., Valente, E. & Mondillo, N. (2023) Spatial distribution of rock uplift in the Bongarà district (Peruvian Andes) and implications for the genesis of supergene ore deposits. *Geomorphology*, 439, 108861. Available from: https://doi.org/10.1016/j.geomorph.2023.108861

Tarquini, S., Tarquini, S., Isola, I., Favalli, M., Mazzarini, F., Bisson, M., et al. (2007) TINITALY/01: a new triangular irregular network of Italy. *Annals of Geophysics*, 50(3), 407–425. Available from: https://doi.org/10.4401/ag-4424

Tarquini, S., Vinci, S., Favalli, M., Doumaz, F., Fornaciai, A. & Nannipieri, L. (2012) Release of a 10-m-resolution DEM for the Italian territory: comparison with global-coverage DEMs and anaglyph-mode exploration via the web. *Computational Geosciences*, 38(1), 168–170. Available from: https://doi.org/10.1016/j.cageo.2011.04.018

Totaro, F., Petrosino, P., Valente, E., Arienzo, I., D'Antonio, M., Di Vito, M. A., Giaccio, B., Jicha, B. R., Petrelli, M., Santangelo, N., Santo, A., & Zanchetta, G. (2024). Last interglacial paleoshoreline location and tectono-stratigraphic evolution of the peri-Tyrrhenian Sarno basin, southern Italy, constrained by tephrostratigraphy. *Earth Surface Processes and Landforms*. https://doi.org/10.1002/esp.6039

Valente, E., Allocca, V., Riccardi, U., Camanni, G. & Di Martire, D. (2021) Studying a subsiding urbanized area from a multidisciplinary

perspective: the inner sector of the Sarno plain (southern Apennines, Italy). *Remote Sensing*, 13(16), 3323. Available from: https://doi.org/10.3390/rs13163323

Valente, E., Ascione, A., Santangelo, N. & Santo, A. (2019) Late Quaternary geomorphological evolution and evidence of post-Campania ignimbrite (40ka) fault activity in the inner sector of the Sarno plain (southern Apennines, Italy). *Alpine and Mediterranean Quaternary*, 32, 185–197. Available from: https://doi.org/10.26382/AM

Varzi, A.G., Meschis, M., Fallati, L., Scicchitano, G., De Santis, V., Scardino, G., et al. (2024) New chronology for submerged relict paleoshorelines and associated rates of crustal vertical movements offshore the Marzamemi village, Sicily (southern Italy). *Marine Geology*, 474, 107326. Available from: https://doi.org/10.1016/j.margeo.2024.107326

Wells, D.L. & Coppersmith, K.J. (1994) New empirical relationships among magnitude, rupture length, rupture width, rupture area, and surface displacement. *Bulletin of the Seismological Society of America*, 84(4), 974–1002. Available from: https://doi.org/10.1785/BSSA0840040974

Westaway, R. (1993) Quaternary uplift of southern Italy. *Journal of Geophysical Research*, 98(93), 21741–21772. Available from: https://doi.org/10.1029/93JB01566

SUPPORTING INFORMATION

Additional supporting information can be found online in the Supporting Information section at the end of this article.

How to cite this article: Cerrone, C., Meschis, M., Ascione, A., Soligo, M., Tuccimei, P., Robertson, J. et al. (2025) Tectonic implications of raised Quaternary relative sea-level indicators along the NE border of the Campania Plain (southern Italy). *Earth Surface Processes and Landforms*, 50(1), e6066. Available from: https://doi.org/10.1002/esp.6066